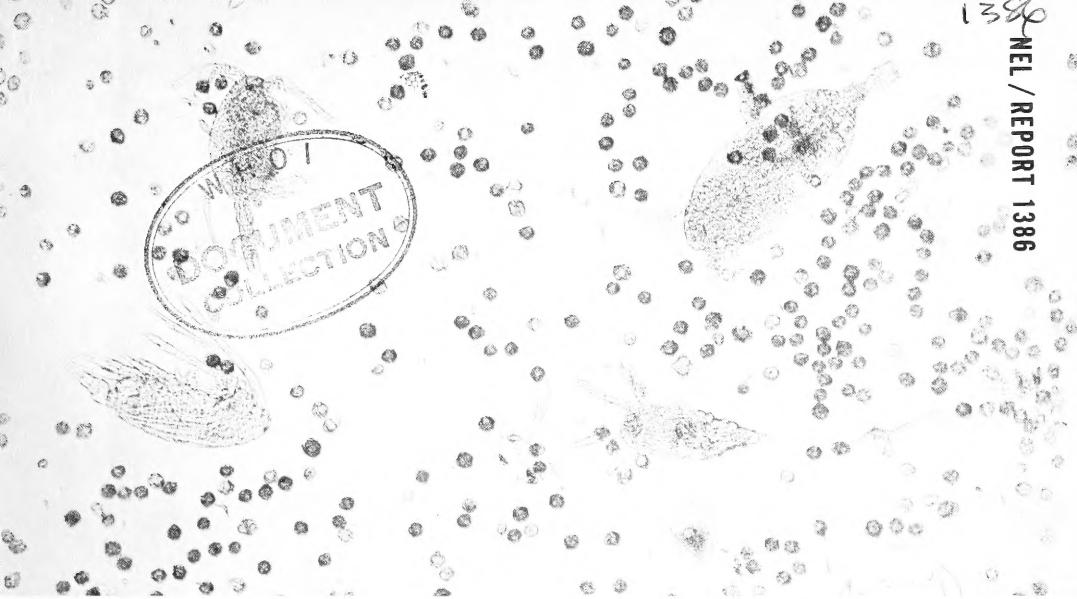

PLANKTON AND TURBIDITY

An investigation of time and space distribution of microorganisms and other materials producing attenuation of light in the open sea

E. G. Barham,
J. W. Wilton, and M. P. Sullivan • Research and Development Report • 1 July 1966

U. S. NAVY ELECTRONICS LABORATORY, SAN DIEGO, CALIFORNIA 92152

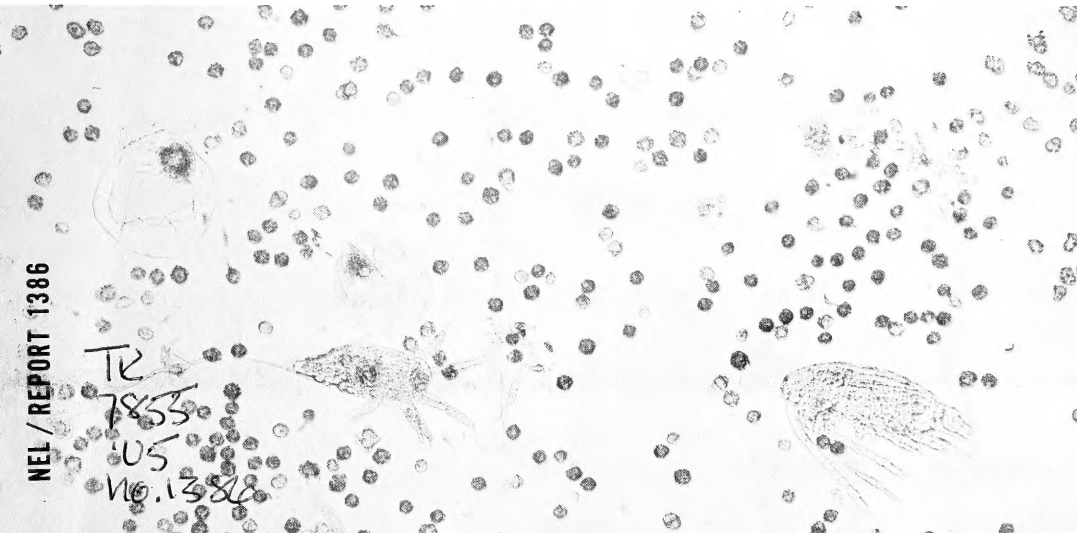

NEL / REPORT 1386

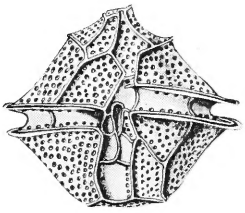

Gonyaulax polyedra

THE PROBLEM

Investigate factors in the marine biological environment which pertain to underwater sound; identify and study organisms affecting sound attenuation, scattering, reflection, and ambient noise level; measure the effects of these organisms on underwater sound. Investigate the distribution of these organisms in space and time to gain an understanding of their fluctuations in critical areas of the ocean.

Specifically, determine the influence of planktonic organisms on the transmission of light in the open sea.

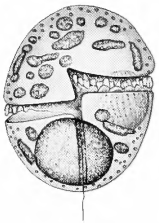

Gymnodinium flavum

RESULTS

1. Unicellular organisms in bloom quantities were found to reduce yellow light transmission in the sea.

2. Light transmission was also reduced by other factors, including organic material, particulate detritus, and dissolved pigments.

3. The time and space distributions of microorganisms and materials producing attenuation of light are complex, but show relationships to thermal structure and water movement caused by currents, tides, internal waves, and surface agitation.

4. The most important of the light-attenuating organisms off Mission Beach, California, in the summer are the dinoflagellates. The greatest concentration of dinoflagellates usually occurs in the water in or above the thermocline.

5. Macroplankton have little effect on light transmission.

RECOMMENDATIONS

1. Use the values of turbidity and the information pertaining to the related abundance of organisms provided in this report when optical or visual operations or installations are required.

2. Study the relation of phytoplankton blooms to physical and chemical phenomena to produce criteria enabling prediction of plankton bloom development and abatement.

3. Investigate the effect of phytoplankton blooms on sound transmission.

4. Correlate diver vision with hydrophotometer measurements and biological populations; investigate the effects of various biological populations on the operation of underwater lasers; measure and correlate bioluminescence with concentrations of dinoflagellates and water transparency.

5. Observe the size, origin, and geographic distribution of colored water masses from airplanes and satellites; establish the relation between light transmission and seasonal blooms of phytoplankton.

ADMINISTRATIVE INFORMATION

Work was performed under SR 104 03 01, Task 0588 (NEL L40961) by members of the Marine Environment Division. The report was approved for publication 1 July 1966.

The authors wish to extend acknowledgments to M. A. Taylor, for aid in data collection and counts of organisms; to H. G. Kiner, for valuable support from the NEL oceanographic research tower; to M. E. Hirst, G. L. Prible, and P. A. Hansen, for assistance in preparation of the graphs; to A. T. Moore, I. E. Davies, and J. L. Cairns, for help with the mathematical analysis; to R. Holmes and Dr. W. Belser, for advice; and to Drs. G. H. Curl and E. C. LaFond, for critically reviewing the manuscript. J. W. Wilton and M. P. Sullivan are summer employees of NEL.

CONTENTS

TABLES

ILLUSTRATIONS

Illustrations (Continued)

Illustrations (Continued)

INTRODUCTION

BACKGROUND

The success of Navy operations utilizing underwater observations by divers, television, or light-emitting devices is limited by the transparency of the water. Optical properties are characteristic of various geographic and oceanic regions, and in some ocean areas reliable predictions can be made concerning the limits of visibility in a given situation. However, inshore temperate regions adjacent to large land masses are subject to great physical and biological changes which affect the color and transparency of seawater and the following factors must be considered: runoff from shore and discharge from rivers bearing pigments, pollutants, and suspended materials; inorganic materials eroded from seacliffs by wave action; effluent from sewer outfalls; tidal and wave scour which roils particulate material into suspension; and the products of organic growth.

In the ocean off semiarid regions such as southern California, many of these factors are reduced in intensity, or exist, if at all, to a negligible degree. It appears, therefore, that organic production -- the life cycles of bacteria, plants, and animals, and the interaction of their metabolic products -- may be the primary source of material reducing transparency in neritic waters within which the Navy must operate.

The development of instruments utilizing photocells stimulated considerable work on the pattern of light transmission in the oceans. (Refer to Holmes, 1957,[1] and Tyler and Preisendorfer, 1962,[2] for review articles.) Further, many studies have been conducted on the suspended organic matter in the seas by using the data as an index of productivity, and in some cases relating them to light-extinction coefficients. (Parsons, 1963,[3] reviews this literature.) Hart, 1962,[4] citing data from 1938 to 1939 taken on the DISCOVERY II cruise, demonstrates a correlation between Secchi disc readings and phytoplankton concentrations. Other qualitative observations indicate that turbidity is frequently associated with phytoplankton populations (Young, 1939;[5]

Burt, 1955;[6] LaFond and Sastry, 1957;[7] Ball and LaFond, 1964;[8] Tyler and Preisendorfer, 1962[2]). However, no quantitative analysis of plankton taken in conjunction with critical transparency measurements, such as is presented in this report, has been found in the literature.

The problem is difficult. Particles both living and inanimate must be analyzed over a wide size range. Sampling must be done frequently enough in time and space to correlate with movements of water masses such as tides, currents, vertical mixing, and turbulence originating at the air-sea interface. For example, Burt, 1955,[6] dealing primarily with inorganic particles with a median radius of 0.3 micron, notes variations in extinction by a factor of 4 during a single half-tidal cycle. Furthermore, turbid zones off the southern California coast are related to internal waves (Ball and LaFond, 1964[8]). Thus, plankton distribution can be just as dynamic in time and space as internal waves.

The relationship between the vertical distribution of phytoplankton and thermal structure is well documented. Gessner (1948),[9] Johnson (1949),[10] and Sorokin (1960)[11] have noted the highest concentration of phytoplankton in or above the thermocline. Ball and LaFond (1964)[8] found the attenuation of light to be associated with thermal gradients and suggested phytoplankton as the causal factor.

PURPOSE

This work attempts to determine the cause of turbidity in a specific location through depth and time with particular emphasis on the role played by living organisms. Consequently, the major portions deal with assessing the concentrations of macroplanktonic and microplanktonic forms and relating them to light transmission and thermal gradients. Inanimate debris above 10 microns is also enumerated.

"Microorganisms" and "microplankton" are defined in this report as unicellular organisms greater than 10 microns and too small in their least dimension to be quantitatively retained by 20-gauge nylon gauze with aperture size of 76 microns. "Macroplankton" refers to organisms retained by 20-gauge nylon gauze to a maximum of 2 mm.

Most of the field work was carried out through two day-night periods during July 1961, and supplementary data were taken in July 1964. The 1961 periods are identified as Operations I and II. During Operation I, 1730 6 July through 1300 7 July, a condition known as "yellow water," caused by a bloom of a small naked dinoflagellate, *Gymnodinium flavum* (Lackey and Clendenning, 1963),[12] provided an excellent opportunity to assess the effect of motile, pigmented cells on light transmission. By Operation II, 0900 20 July through 1200 21 July, the dinoflagellate bloom had abated and a more complex and perhaps more typical situation was present. A third operation was carried out 23, 24 July 1964 during a "red water" bloom caused by the dinoflagellate *Gonyaulax polyedra.*

EQUIPMENT

NEL TOWER

The NEL oceanographic research tower is located approximately 1 mile off Mission Beach, San Diego, California, in 60 feet of water (fig. 1). The sandy bottom recedes gently seaward. Along three sides of the tower, pairs of tracks run vertically from the platform work area to the bottom. Sled-like carts with shoes loosely clamped on the rails are lowered and raised by winches and permit the accurate placement of instruments in the water column. The details of tower construction, instrumentation, and operation are described by LaFond (1959).[13] The use of this fixed, stable platform alleviated many of the sampling problems inherent in shipboard operation by fixing the study in space.

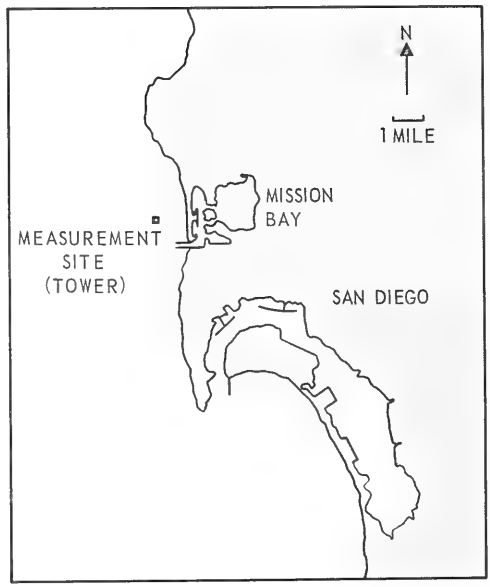

Figure 1. Location of NEL oceanographic research tower.

HYDROPHOTOMETER

Light transmission was measured with a hydrophotometer (fig. 2) developed by J. Tyler, of Scripps Institution of Oceanography Visibility Laboratory. The theory of such instruments is discussed by Tyler and Preisendorfer (1962)[2] and Holmes (1957).[1] The device measured light intensity impinging on a Weston 856-RR photocell. The light was transmitted along a 1/2-meter path from a 6-volt light bulb (General Electric 964). The filament voltage was monitored by a Cohu electronic galvanometer, and a variable power supply was used for calibration. Baffles were placed along the light path to eliminate ambient light. The photocell output was fed to the pen drive of a Leeds and Northrup Speedomax recorder. The hydrophotometer was adjusted

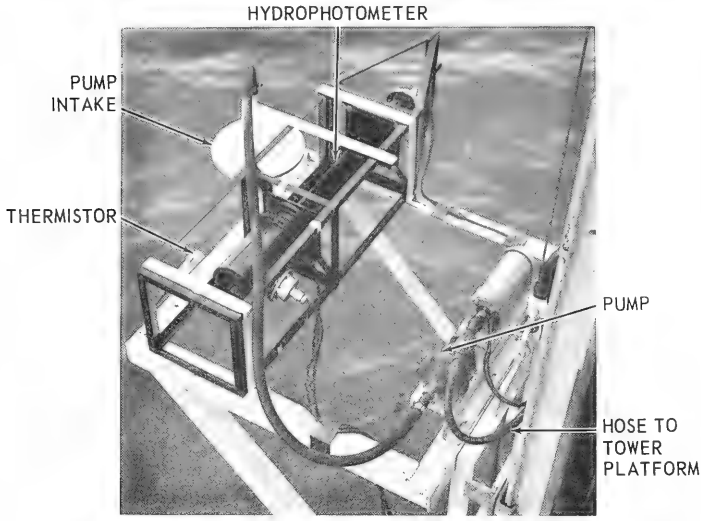

Figure 2. Equipment rack on tower used to measure light transmission, temperature, and depth, and to sample plankton in the water.

to compensate for the natural attenuation of water molecules, and the reading in distilled water was established as 100-percent transmission. Measured light loss in the marine environment is due to a combination of absorption and scatter. The instrument did not discriminate between the two.

TEMPERATURE SENSOR

Temperature was determined prior to each sampling run by a bathythermograph (BT) lowering from surface to bottom and by a thermistor bead sensor on the cart (fig. 2), with galvanometer readout in the instrument hut. The BT data are considered more accurate than the thermistor measurements, and have been used in this report.

UNDERWATER PUMP

Water samples were obtained by a submersible pump. The intake was fitted with plates 1 cm apart (fig. 2), which limited the depth of the stratum sampled to about 10 cm, as demonstrated by experiments with dye. Water was delivered to the platform of the tower through 3/4-inch plastic hose. The pump and hydrophotometer were mounted together on the cart. A meter wheel assured sampling from known depths. Two types of samples were taken to insure adequate sampling of variously sized entities of different degrees of motility and population density.

METHODS

MACROPLANKTON

SAMPLING

The larger and more sparse macroplankton were sampled by the following method. The instrument cart was lowered to within 2 feet of the bottom, time was allowed for the water already present in the hose to be pumped out, and a 5-gallon sample was passed through a plankton net (Kahlsico No. 1520) hung with 20-gauge nylon gauze. Water pumped and filtered was caught and measured in a stainless steel container. The catch concentrated in the cod-end bucket was washed into 8-ounce bottles and fixed in 10-percent formalin.

The procedure was repeated every 10 feet through the water column until six samples were obtained. The last sample was taken 52 feet from the bottom and varied with respect to distance from the sea surface according to tide and wave action. Depth positioning from a fixed platform in a shallow environment is more consistent relative to the bottom than depth positioning from a constantly changing surface. Vertical sampling series for macroplankton took about 30 minutes.

FIXING AND COUNTING

The formalin-fixed macroplankton samples were concentrated through a piece of 20-gauge nylon netting identical to that used in the net and backwashed into 10-ml attenuated centrifuge tubes (fig. 3). When the samples had settled for about 1 hour, the wet displacement was measured and the material withdrawn in a large-bore pipette. Placed in a long plastic trough (fig. 4), the entire sample was counted under a magnification of 23 diameters. At this power, the width of the trough is slightly less than the

diameter of the field of vision. Thus, the entire sample was distributed linearly within the width of one field of view. The trough was passed slowly under the scope and the catch was identified and counted. This procedure increased the accuracy of counting and the speed of analysis.

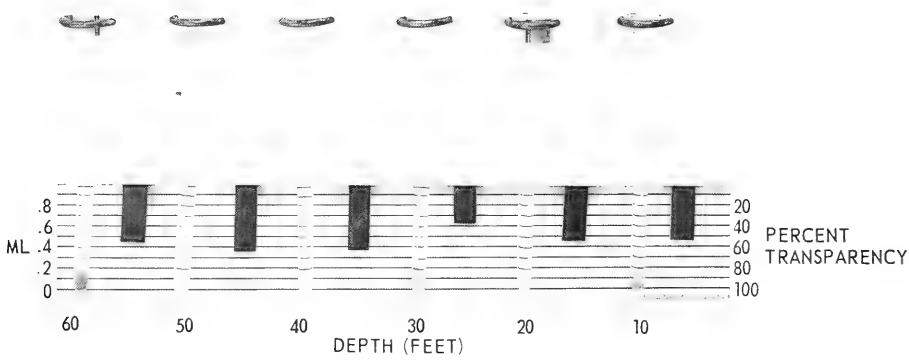

Figure 3. Vertical series of filtered material concentrated at the bottom of centrifuge tubes (volume displacement) and related turbidity of water.

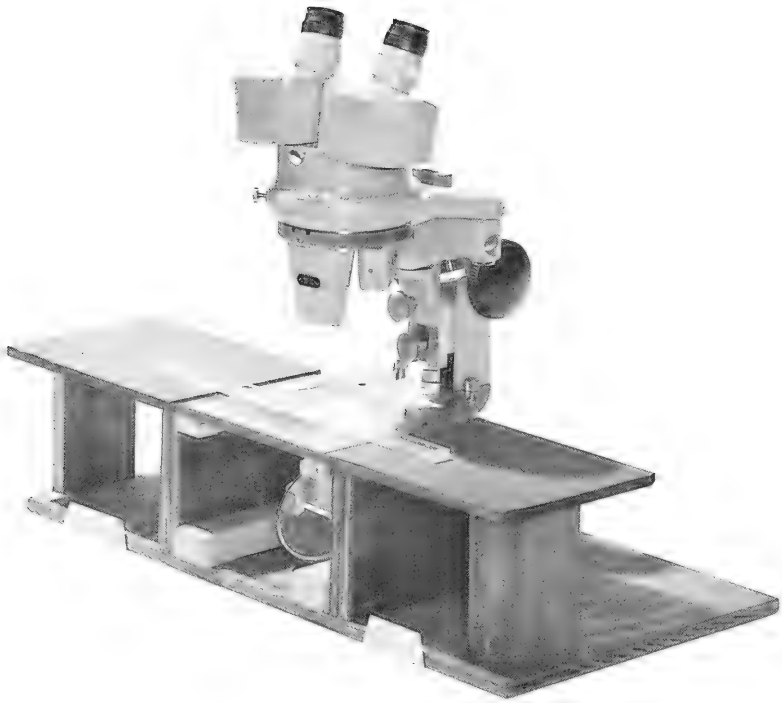

Figure 4. Microscope and plastic trough used in macroplankton counts.

MICROPLANKTON

SAMPLING

An operation designed to obtain the smaller, denser microplankton immediately followed each sampling of macroplankton. The instrument cart was again lowered to the bottom, the pump cleared, and the cart drawn to the surface without stopping.

During these runs, the pump and hydrophotometer were in constant operation. Depth of sampling was computed from the rate of ascent of the instrument cart and the time-lag necessary for water delivery. Six 8-ounce bottles were filled with water from approximately the same depths as the macroplankton samples and the organisms were fixed with Lugol's iodine. Microplankton samples for each vertical series were taken in approximately 3 minutes.

PREPARATION OF SLIDES

With the exception of the stains used, microconstituents were prepared by the technique reported by Holmes (1962).[14] The sample was thoroughly agitated, and a 20-ml aliquot was removed and introduced into a Millipore filter apparatus. The aliquot was drawn through an HA Millipore Filter, pore size 0.45 micron ±0.02 micron, under pressure of 10 to 11 psi. Salts were removed by passing a series of increasingly dilute seawater-distilled water solutions through the filter membrane. The filter was rinsed with distilled water and stained with a saturated aqueous solution of Safranine "O" for 20 minutes. The sample was dehydrated with increasing concentrations of ethanol in distilled water. Between applications of the 75- and 100-percent solutions of alcohol, the sample was counter-stained with a saturated solution of Light Green in 95-percent ethanol for 5 to 6 seconds. The filter was cleared with beechwood creosote and mounted on slides with Canada balsam. For these operations a manifold (fig. 5) was fabricated which permitted the simultaneous preparation of six samples. In practice,

Figure 5. Manifold used in Millipore filtration to prepare slides of microorganisms.

however, it was found that it was most efficient to prepare no more than two samples at a time.

COUNTING

Microplankton counts were made under a compound microscope at 200 diameters. Size estimates of all organisms greater than 10 microns in diameter were made with a Whipple ocular disc. The collecting area of the mounted filter membrane was fixed by the diameter of the Millipore apparatus. The diameter of the collecting area was found to contain 36 square fields (fig. 6) delineated by the grid of the Whipple ocular disc. The total number of fields per slide was computed; each slide had a total area of 1017 fields.

Concentrations as great as 10^3 per ml of microconstituents made total counts, which had been made in the analysis of macroplankton, impractical. Consequently, a valid sampling technique had to be developed for microconstituents. Counts of all recognizable organisms, together with inorganic particles and debris 10 microns or larger, were made by means of a random-sampling technique. Organisms in five percent (51 fields) and in $2\frac{1}{2}$ percent (25 fields) of the collecting area were counted. The following method was used. All particles contained in 1 field, 25 fields, and 50 fields were counted and recorded by two people. Each count by each person was repeated 10 times. Variation in results of one individual's counts and differences between results obtained by the two individuals were analyzed. Both comparisons revealed differences in the number of organisms which approached 20 percent in isolated instances. In every case, however, the rank order of particles remained the same. The largest difference in counts involved those particles which were either present in large numbers, such as *Gymnodinium flavum*, or were not only numerous but also difficult to recognize. A further difficulty was that the distribution of particles following Millipore filtration is not even. Clumping of organisms and apparent adsorption of particles to glass filtration tubes tend to form a ring on the filter, a difficulty also encountered by Holmes (1962).[14] Whereas most counts were within 12 percent, no greater

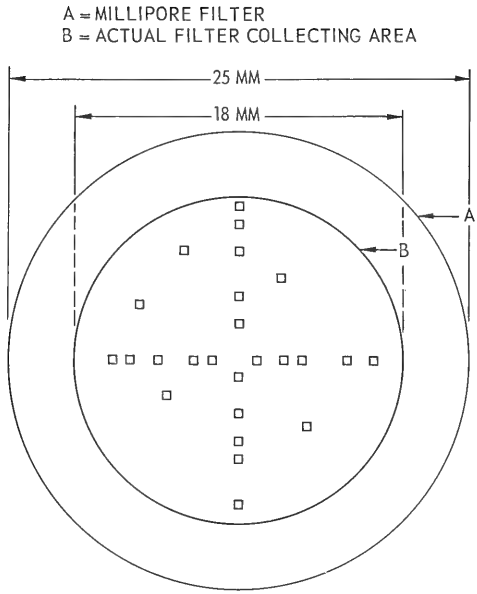

Figure 6. Diagram illustrating counting technique used for microplankton. Each square depicts the field of the microscope as delineated by the Whipple ocular disc. Collectively the squares indicate a typical count in which ten fields were counted as the slide was moved transversely in each of two directions. Five additional fields were selected at random from the remaining quadrants, making a total of 25 (2½ percent) fields counted.

accuracy than ±20 percent for the analysis is assumed. This is about as accurate as chlorophyll extraction (Richards and Thompson, 1952),[15] but is not as critical as gravimetric methods of microplankton analysis (Banse *et al.*, 1963).[16] It was found that the margin of error was not significantly different between the 5-percent and the $2\frac{1}{2}$-percent counts; therefore, $2\frac{1}{2}$ percent of the fields on each slide were counted. Counts were made by the method illustrated in figure 6.

DATA REDUCTION AND PRESENTATION

The various materials in the water are divided into three categories -- macroorganisms, microorganisms, and inanimate particles. The categories are related to turbidity and temperature structure. The maximum and minimum counts are listed in tables 1 and 2.

Time-depth plots were prepared to show the relative concentrations of organisms. Because the organisms varied greatly in concentration, an exponential contouring interval was established which differs from organism to organism. The highest count of each organism or entity per liter or milliliter of water for each operation was taken, and about 5 percent of it was used as a base number to establish a contouring interval. Contour intervals were established by successively doubling the base number to depict ascending magnitudes of population. The number of organisms per liter was entered for each sample at the corresponding time and space, and the above percentages were interpolated and contoured. On occasions where they aided interpretation of the data 50-percent increments in population density were used. These increments appear on the charts as broken lines.

Light transmission, corresponding in time and depth to the water samples, was plotted, and the percentages were interpolated. Comparisons were made between transmission readings taken at the times of microplankton and macroplankton runs. The same general patterns were apparent. Because a lack of correlation between macroplankton and transparency data was evident, and to reduce the number of figures, only light measurements made at the time of microplankton runs are presented in the text. Transparency charts taken at the time of the macroplankton runs are in the appendix. Transparency data for both operations have been superimposed on distribution charts. Depth scales are given in reference to the mean tide level. Depth of any sample or observation may be obtained by applying these scales to the surface line.

TABLE 1. MICROENTITIES RELATED TO TURBIDITY, OPERATION I.

Organisms	Fig.	Size*		Range (Numbers per ml)	With Photosynthetic Pigments
		Range (Microns)	Average (Microns)		
Gymnodinium flavum	12	14–33 (diam)	28.8	54–3872	+
Ceratium fusus	13	182–218 (long) 23.6–36.6 (wide)	200 × 28.3	0–214	+
Ceratium furca	14	100–135 (long) 36.3–46.8 (wide)	118 × 44.5	2–88	+
Other dinoflagellates	15	15–40 (diam)	N.M.**	6–144	+
Diatoms	16	N.M.	N.M.	0–82	+
Total microorganisms	17	N.M.	N.M.	144–4130	+
Nonliving particles					
Organic aggregates	A-2	10–25	N.M.	6–118	–
Wood fibers	A-3	10–500	N.M.	0–42	–
Unidentified particles	A-4	10–500	N.M.	96–860	–
Total inanimate particles	18	10–500	N.M.	122–940	–
Organisms and inanimate particles					
Total microconstituents	19	10–218	N.M.	386–4416	±

*Measurements made on fixed material

**Not measured

TABLE 2. MICROENTITIES RELATED TO TURBIDITY, OPERATION II.

Organisms	Fig.	Size*		Range (Numbers per ml)	With Photosynthetic Pigments
		Range (Microns)	Average (Microns)		
Gymnodinium flavum	23	14–33 (diam)	28.8	12–856	+
Ceratium fusus	24	182–218 (long) 23.6–36.6 (wide)	200 × 28.3	2–202	+
Ceratium furca	25	100–135 (long) 36.3–46.8 (wide)	118 (long) 44.5 (wide)	0–80	+
Other dinoflagellates	26	15–40 (diam)	N.M.**	2–90	+
Diatoms	27	N.M.	N.M.	0–6	+
Total microorganisms	28	N.M.	N.M.	72–972	+
Nonliving particles					−
Organic aggregates	A-10	10–25	N.M.	38–184	−
Wood fibers	A-11	10–500	N.M.	0–184	−
Unidentified particles	A-12	10–500	N.M.	244–800	−
Total inanimate particles	29	10–500	N.M.	310–984	−
Organisms and inanimate particles					
Total microconstituents	30	10–218	N.M.	674–1918	±

*Measurements made on fixed material

**Not measured

MACROORGANISMS

The principal macroorganisms present in both operations were nauplii (larvae), copepods, and polychaete worm larvae. Generally, nauplii were most numerous, with copepods and polychaetes following in that order. Figures illustrating the distributions of these organisms in time and space are found in the appendix. Cladocerans, chaetognaths, bivalve larvae, and rotifers were also present in low numbers, but were not plotted. The lack of correlation between macroorganisms and light attenuation cited previously is treated in DISCUSSION. The nature and size of characteristic plankton types are shown in figure 7.

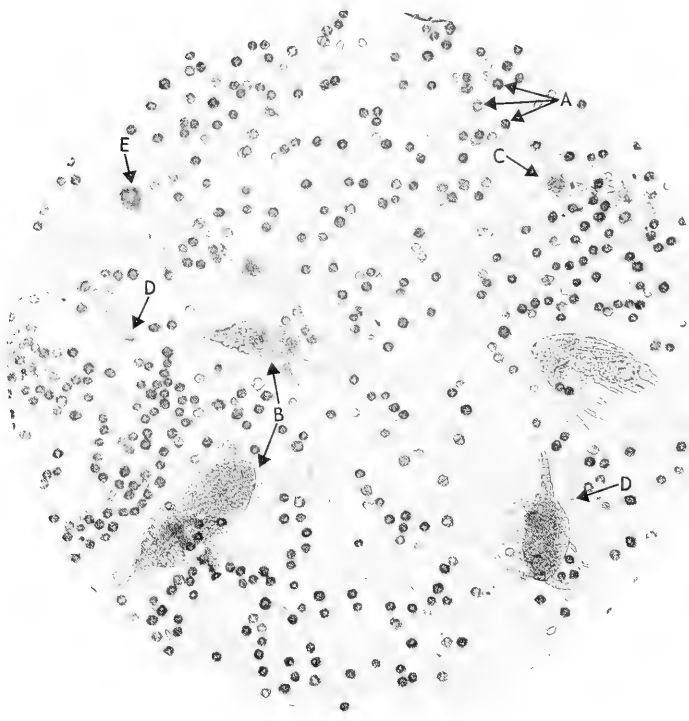

Figure 7. Typical planktonic organisms. A. *Gonyaulax polyedra*, B. Immature copepods, C. Tintinnids (a testiculate protozoan), D. *Ceratium* species, E. Naked dinoflagellate.

MICROCONSTITUENTS

MICROORGANISMS

Five categories of microorganisms (tables 1 and 2) were counted. The sum of the five concentrations is tabulated under "Total microorganisms." For each entry in each operation a time-depth plot of population density was prepared.

Three species of dinoflagellates were prevalent, with *Gymnodinium flavum* dominant during both operations. This organism is essentially a sphere averaging 28.8 microns in diameter after fixation. Two species of *Ceratium*, tentatively identified as *C. furca* and *C. fusus*, were common. *C. furca* averaged 123.0 microns in length by 53.1 microns in width, and *C. fusus* averaged 188.0 microns in length by 29.5 microns in width.

The heading "Other dinoflagellates" combines in one category dinoflagellates not numerous enough to consider individually. The cells are generally spherical and vary between 15 and 40 microns in diameter.

Several species of diatoms were in evidence; individually never in high concentration, they are lumped for treatment.

INANIMATE PARTICLES

Nonliving particles over 10 microns are grouped in several categories. Fibrous material is tabulated under "Wood fibers." Fecal-like particles appear under "Organic aggregates," and other detritus is summarized under "Unidentified particles." The sum of "Total microorganisms" and "Total inanimate material" makes up "Total microconstituents."

MATHEMATICAL TREATMENT

This study is based on the assumption that organisms in the water will reduce the intensity of a beam of light. By considering their sizes and population density in the volume of water through which the light passes, we should be able to treat the problem mathematically. By the method of least squares, lines were computed for the scatter diagrams depicting the numbers of organisms or entities versus light transmission for *Gymnodinium flavum* and total microconstituents, Operations I and II (fig. 8).

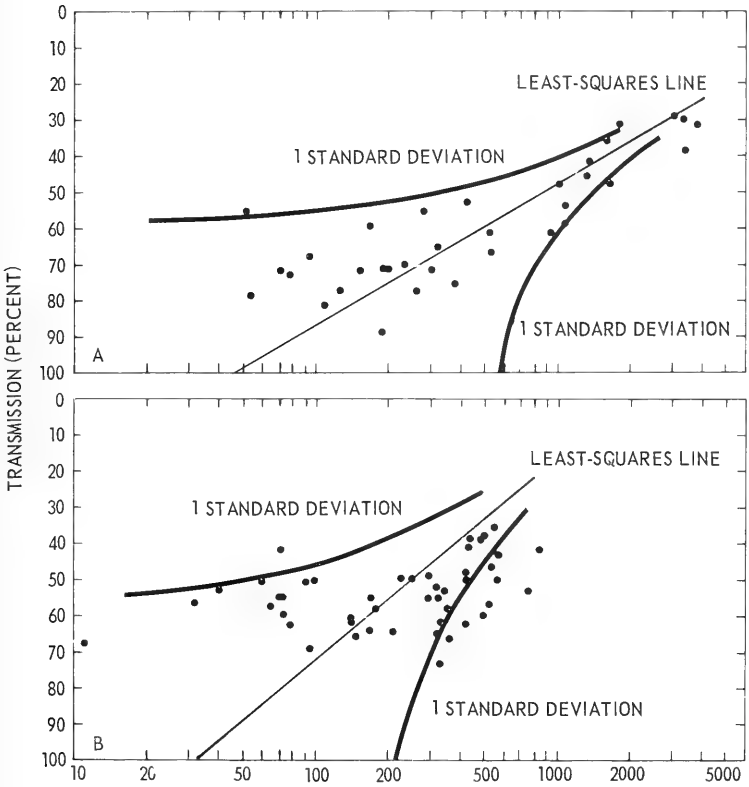

Figure 8. Least-squares lines illustrating the relationship between light attenuation and number of microentities. A. *Gymnodinium flavum*, Operation I, B. *Gymnodinium flavum*, Operation II.

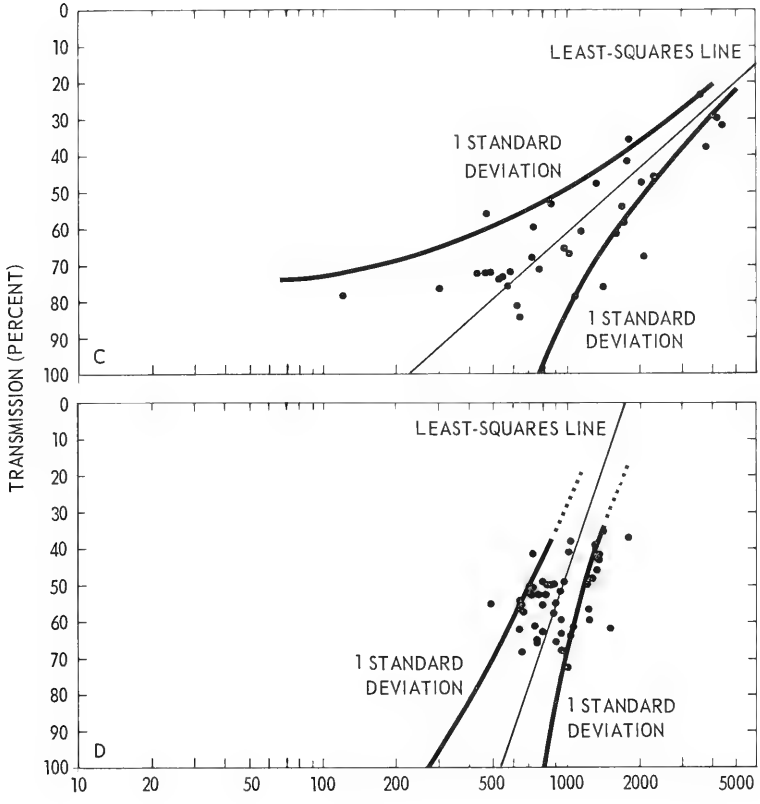

Figure 8 (continued). C. Total microconstituents, Operation I, D. Total microconstituents, Operation II.

TOTAL CELL SURFACE AREA AND LIGHT ATTENUATION

From the highest count and an assumed mean cell diameter of 30 microns, the total cross-sectional area of *Gymnodinium flavum* in the volume of water represented by the cylindrical light path, 1.9 cm in diameter by 50 cm in length, was computed. This figure, 3.87 cm^2, exceeded the cross-sectional area of the light path, 2.83 cm^2, by more than 36 percent. It supplied a rough estimate of light-intercepting capacity, but assumed a nonrandom distribution and neglected scatter and selective absorption.

THEORETICAL MODEL FOR DETERMINING POPULATION DENSITIES OF UNICELLULAR FORMS

A theoretical model for determining the population density of single-celled forms using size data for *Gymnodinium flavum* and based on light absorption was constructed. Four assumptions were made to construct the model and to derive curves which were compared to scatter diagrams of *Gymnodinium flavum* and total microconstituents in both operations. While each of them was recognized as being a rough approximation, the calculation was of interest as a possible indication of relationships between unicellular forms and light attenuation. Furthermore, as the number of organisms N increases, the situation should more nearly approximate the assumptions.

If the ratio of light received by a hydrophotometer photocell to that emitted by the light source is known, it is possible, with the following assumptions, to calculate the number of organisms present within the light beam. The assumptions are:

1. Only one type of organism or light-absorbing entity is present in the beam and its average cross-sectional area is known.

2. The organisms are optically black, and no diffraction occurs at their boundaries.

3. The organisms are randomly distributed within the beam.

The following calculations were made: If α equals the average absorption cross-sectional area of the individual organism, β the cross-sectional area of the light path, and γ the total cross-sectional area blocked by all the organisms, then $\frac{\gamma}{\beta}$ represents the fraction of the beam blocked by all organisms present and $\frac{\beta-\gamma}{\beta}$ represents the unblocked fraction of the emitted light which reaches the photocell. Since $\frac{\beta-\gamma}{\beta}$ and β are known, it is necessary only to calculate $\gamma = F(N,\alpha,\beta)$ to determine N, the number of organisms within the beam. The approach to determining $\gamma = F(N,\alpha,\beta)$ is statistical.

If only one organism is present in the beam, then the probability of its blocking out light equal to its own area is 1, and the area it blocks is α. Thus, for $N = 1$, $\gamma = \alpha$. The probability of a second organism's blocking exactly its own area is no longer 1 because of the presence of the first, but is $\frac{\beta-\alpha}{\beta} = 1 - \frac{\alpha}{\beta}$, which is nearly, but not quite, equal to 1. If $\frac{\alpha}{\beta} = \zeta$, then the probable area blocked by the second organism is $\alpha(1-\zeta)$ and for $N = 2$, $\gamma = \alpha+\alpha(1-\zeta)$.

The probability that the third organism will block out exactly its own area is, by the same reasoning,

$\frac{\beta - \{\alpha+\alpha(1-\zeta)\}}{\beta} = 1 - \zeta(2-\zeta)$. The probable area which it blocks out is then $\alpha\{1 - \zeta(2-\zeta)\}$. Thus, $N = 3$, $\gamma = \alpha+\alpha(1-\zeta) + \alpha(1-2\zeta+\zeta^2)$, or for $N = 3$, $\gamma = \alpha\{1 + (1-\zeta) + (1-\zeta)^2\}$. Higher values of N yield the following areas:

N	$P(\alpha)$	$\gamma = F(N,\alpha)$
1	1	α
2	$(1-\zeta)$	$\alpha+\alpha(1-\zeta)$
3	$(1-\zeta)^2$	$\alpha+\alpha(1-\zeta) + \alpha(1-\zeta)^2$
4	$(1-\zeta)^3$	$\alpha+\alpha(1-\zeta) + \alpha(1-\zeta)^2 + \alpha(1-\zeta)^3$
.	.	.
.	.	.
.	.	.
.	.	.
N	$(1-\zeta)^{N-1}$	$\alpha\sum_{I=0}^{N-1}(1-\zeta)^I$

Thus, for any number of randomly distributed organisms N within the beam, the total amount of the beam's cross-sectional area which they will block out is

$$\gamma(\alpha,N) = \alpha\sum_{I=0}^{N-1}(1-\zeta)^I$$

Given a hydrophotometer reading of received light fraction K (or 100 K percent transmitted), we have

$$K = \frac{\beta-\gamma}{\beta}$$

or

$$\gamma = \beta(1-K) = \alpha\sum_{I=0}^{N-1}(1-\zeta)^I$$

or

$$K = 1 - \frac{\alpha}{\beta}\sum_{I=0}^{N-1}(1-\zeta)^I$$

Using a computer, we may now calculate N. The number of organisms per unit volume of water can be calculated by dividing N by the volume of the light beams. Figure 9 illustrates the theoretical curves (100-percent cell number) derived from the foregoing computations. In this treatment the assumption has been made that *Gymnodinium flavum* was the only light absorber, whereas this organism comprised about 65 percent of total microconstituents. Therefore, the curve for 65 percent of the theoretical 100-percent cell number is also shown for comparison with the plotted *Gymnodinium flavum* transparency data (fig. 9A).

Figure 9. Theoretical relationship between light attenuation and number of microentities as determined by a mathematical model for predicting population densities by light attenuation. A. *Gymnodinium flavum*, Operation I, B. *Gymnodinium flavum*, Operation II, C. Total microconstituents, Operation I, D. Total microconstituents, Operation II.

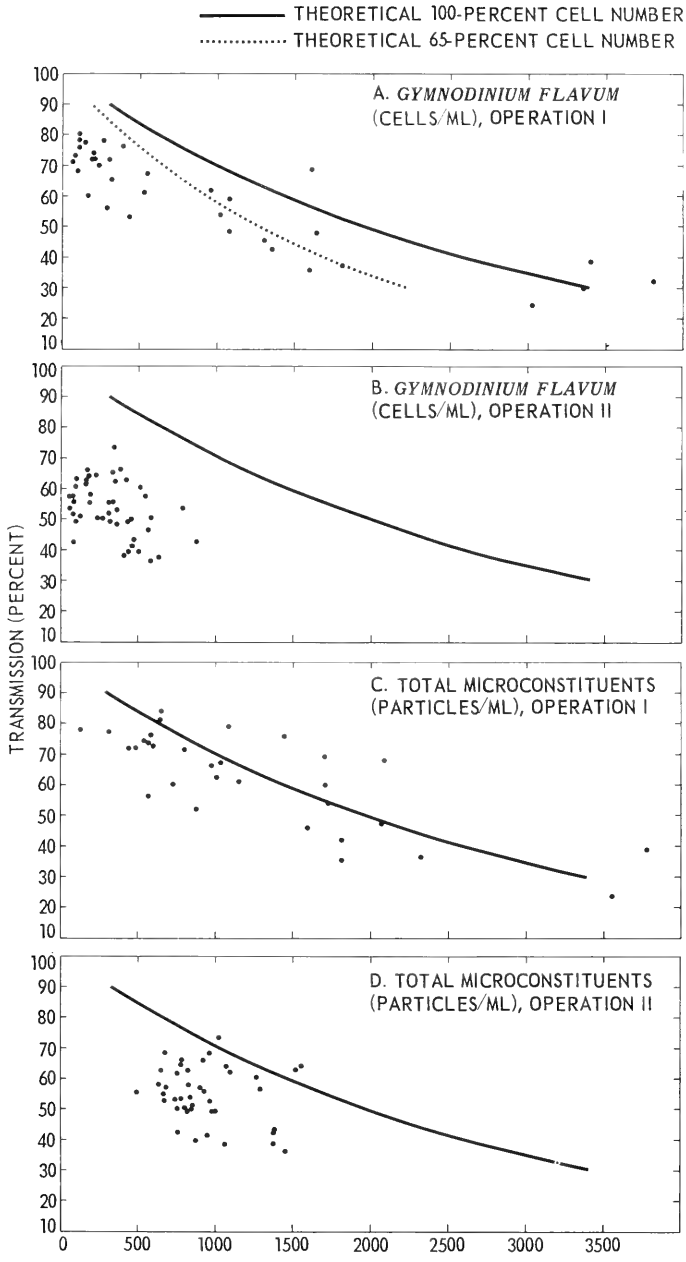
THEORETICAL 100-PERCENT CELL NUMBER
THEORETICAL 65-PERCENT CELL NUMBER
A. GYMNODINIUM FLAVUM (CELLS/ML), OPERATION I
B. GYMNODINIUM FLAVUM (CELLS/ML), OPERATION II
C. TOTAL MICROCONSTITUENTS (PARTICLES/ML), OPERATION I
D. TOTAL MICROCONSTITUENTS (PARTICLES/ML), OPERATION II
TRANSMISSION (PERCENT)
100
90
80
70
60
50
40
30
20
10
0
500
1000
1500
2000
2500
3000
3500

RESULTS

OPERATION I

TURBIDITY

During Operation I, turbid water, with light transmission 50 percent and less, was confined in a layer approximately 12 to 30 feet thick (fig. 10). The maximum turbidity was at 38 feet at 1800 and moved upward during the night to center above 20 feet. From this point the turbid layer thickened, 50-percent water reaching a depth of 30 feet, then again rose toward the surface as observations were terminated. Light transmission during this operation ranged from less than 30 percent (extremely dirty water) to over 80 percent (relatively clear water). During the period of observations transparency values for water near the surface fluctuated from 30 to 72 percent. Bottom readings were characterized by clearest water with transparency values considerably over 50 percent.

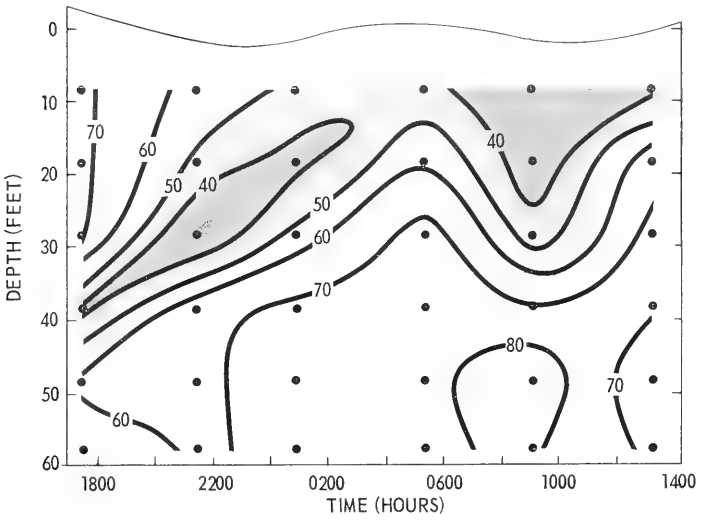

Figure 10. Water transparency (percent transmission), Operation I.

TEMPERATURE

Temperature (fig. 11) ranged from less than 56°F at the bottom to greater than 68°F at the surface. The thermal structure is plotted from BT's with reference to the surface, but referred to, as in the case of turbidity and plankton, with reference to mean sea level. A thermocline was present (60 to 64°F isotherms) throughout this operation. The middle isotherm of the thermocline, 62°F, was at 42 feet at 1800 and at 18 feet at 0500. At this point the thermocline, as indicated by the 62°F isotherm, moved to 42 feet at 0900. The peak of this oscillation, or the shallowest thermocline, occurs about 0500; the deepest thermocline occurs late in the afternoon. This typical cycle is caused by diurnal wind changes.

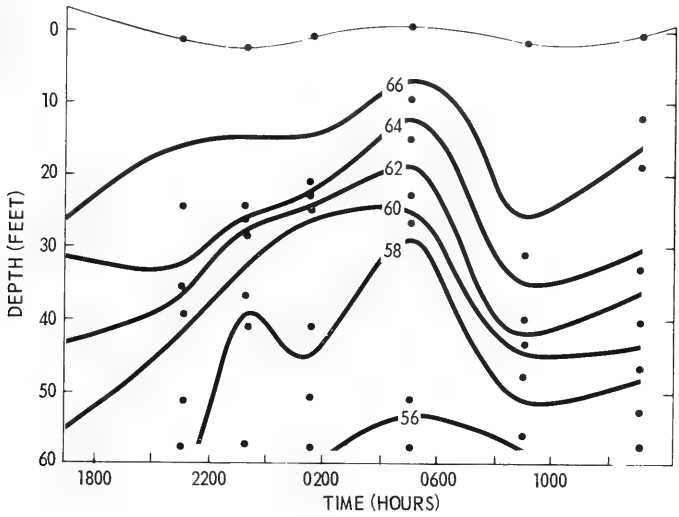

Figure 11. Water temperature (°F), Operation I.

By comparing the temperature structure (fig. 11) with turbidity distribution (fig. 10), we see that the changing level of maximum turbidity lies just above the maximum temperature gradient. Because the salinity gradients in this area are negligible in the summer (less than 0.004 parts per thousand per foot), the temperature gradients correspond to the density gradients. Thus, during this operation, the greatest concentration of organisms tended to occur just above the maximum density gradient.

DISTRIBUTION OF MICROENTITIES IN RELATION TO PHYSICAL FACTORS

The two operations in 1961 were separated in time by 2 weeks and were characterized by different physical conditions and a corresponding difference in distributional patterns of entities related to turbidity. Comparisons between distributional patterns of microentities, light transmission, and temperature revealed some of the interrelationships present in a marine environment. In the following discussion, each microorganism is related to turbidity and temperature for Operation I.

TURBIDITY AND THE DISTRIBUTION OF PARTICLES

Gymnodinium flavum: Similarities in time and space were present between light transmission and the distributional pattern of *G. flavum* (fig. 12). The areas of highest concentration of *G. flavum* fell within the 40-percent transmission contours. Decreases in concentration correlated with increases in illumination. Light transmission of 60 percent and greater is marked by a decrease in cell count from 1200 per ml to 200 per ml.

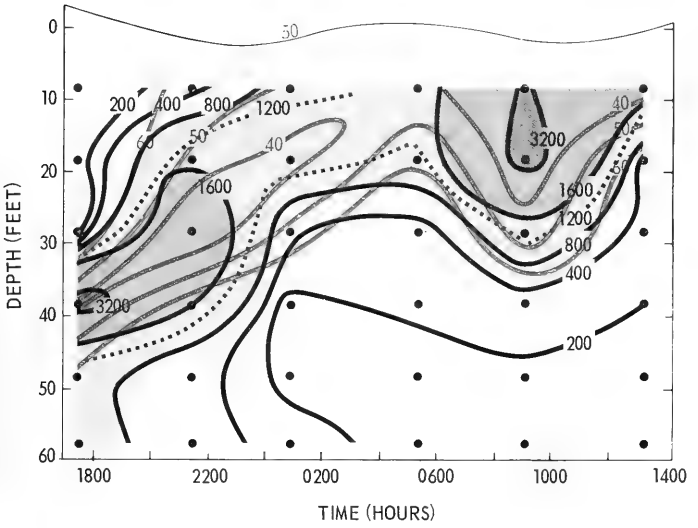

Figure 12. Distribution of *Gymnodinium flavum* (organisms per ml), with transparency data (percent transmission) in red, Operation I.

Ceratium fusus: Cell counts of *C. fusus* (fig. 13) are highest at 28 feet 2100 6 July and 8 feet 0900 7 July. These zones of highest concentration fell within the 60-percent transmission contours. Virtually the entire distribution of *C. fusus* was concentrated between the 40-percent transmission contours. While cell counts are considerably below those of *G. flavum,* this organism probably contributed to light attenuation in an additive fashion.

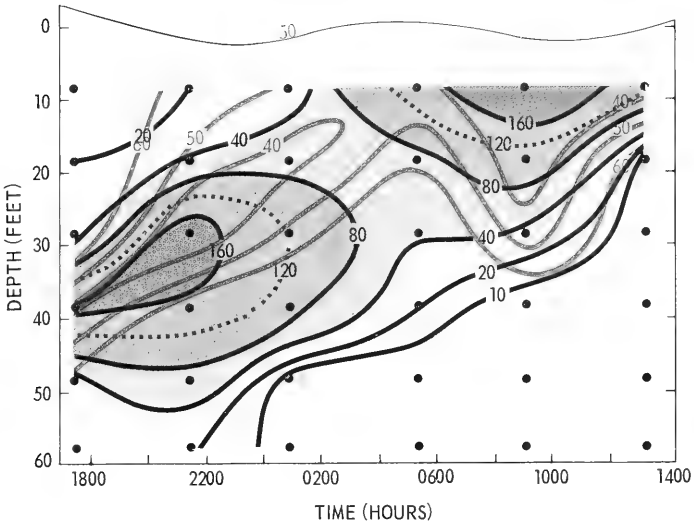

Figure 13. Distribution of *Ceratium fusus* (organisms per ml), with transparency data (percent transmission) in red, Operation I.

Ceratium furca: The distribution of *C. furca* (fig. 14) is similar to that of *C. fusus*. Points of highest concentration were found at 28 feet 2100 6 July, 8 feet 0900 7 July, and 48 feet 1300 7 July. The centers of the first two concentrations were within the most turbid areas and probably contributed to light attenuation in the same fashion as *C. fusus*. However, the near-bottom concentration at 48 feet 1300 7 July was in water showing 70-percent transmission. Thus, this isolated maximum had little effect on light transmission.

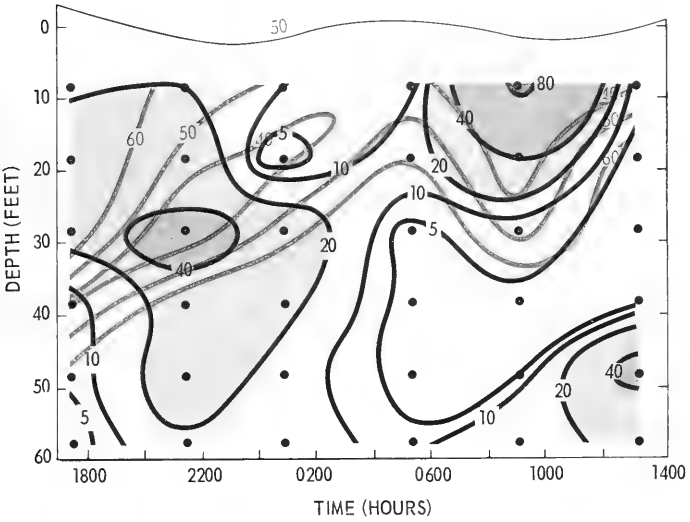

Figure 14. Distribution of *Ceratium furca* (organisms per ml), with transparency data (percent transmission) in red, Operation I.

OTHER DINOFLAGELLATES: The collective distribution of several additional species of dinoflagellates, both armored and naked, is shown in figure 15. Points of population maxima are generally within the most turbid zones. These organisms may have been minor contributors to turbidity, but the presence of populations of the order of 60 cells per ml in clear water of 60-to-70-percent transparency near the bottom from 2000 6 July to 0200 7 July indicates that such cells must be in greater concentrations before light transmission is greatly affected.

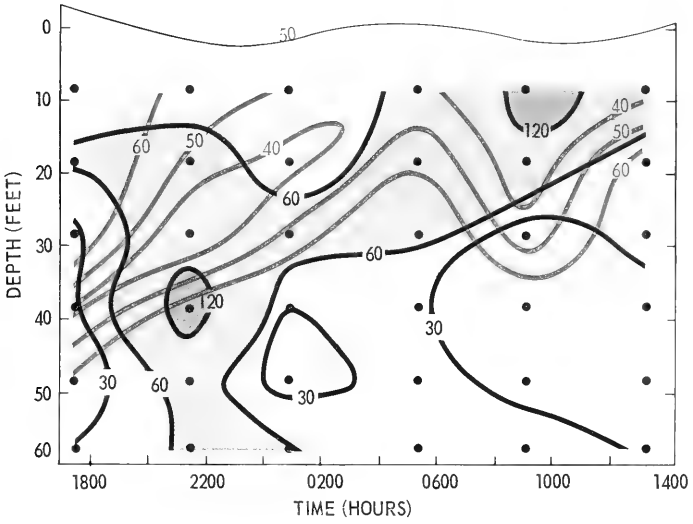

Figure 15. Distribution of other dinoflagellates (organisms per ml), with transparency data (percent transmission) in red, Operation I.

DIATOMS: The accumulated total of several species of diatoms is represented in figure 16. The highest concentration was present near the bottom at 2400 6 July. From this point the concentration decreased toward the surface to 8 cells per ml at 35 feet between 1800 6 July and 0600 7 July. In general, the distribution of diatoms was limited to water which showed 60-percent light transmission or higher. Diatom blooms characteristically occur in the spring in these waters. It is believed the low concentrations found represented the frustules of dead cells, the remnants of previous blooms. Their presence in low numbers made no apparent contribution to light attenuation.

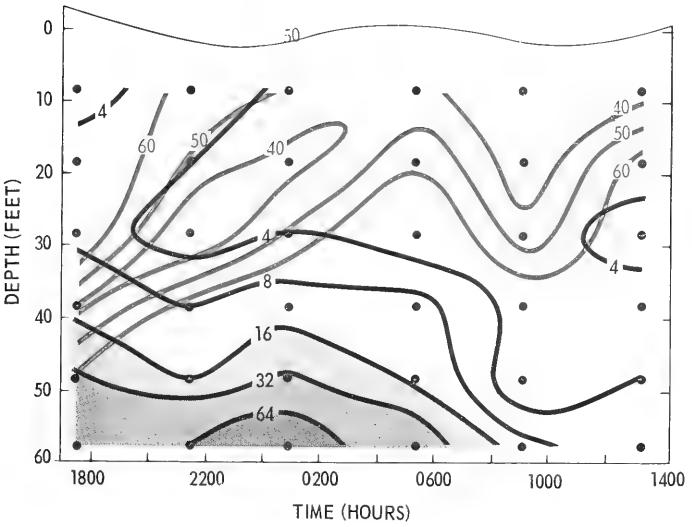

Figure 16. Distribution of miscellaneous diatoms (organisms per ml), with transparency data (percent transmission) in red, Operation I.

TOTAL MICROORGANISMS: Because the concentration of *Gymnodinium flavum* represented 86 percent of the total microorganisms found, the distribution of total microorganisms (fig. 17) closely parallels that of *G. flavum*. The correlation in time and space between *G. flavum*, total microorganisms, and transmission of light clearly implicated *G. flavum* as the major cause of turbidity during this operation.

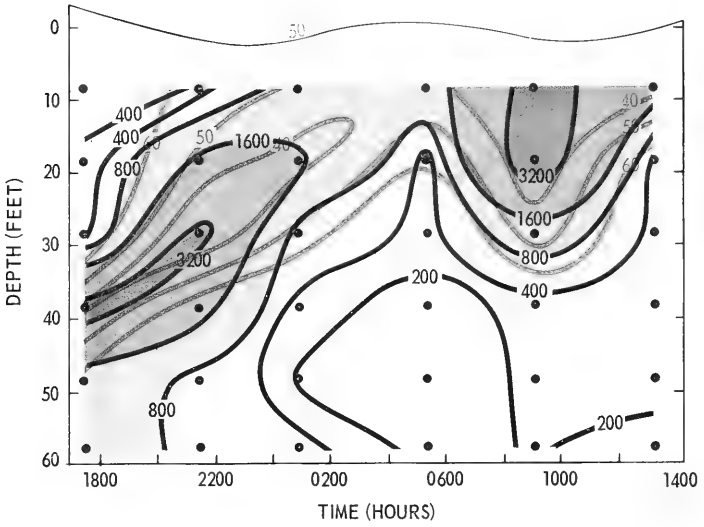

Figure 17. Distribution of total microorganisms (organisms per ml), with transparency data (percent transmission) in red, Operation I.

TOTAL INANIMATE MATERIAL: Figure 18 represents the sum of fecal pellets, wood fibers, and miscellaneous debris over 10 microns in diameter. The distribution of these individual entities is shown in the appendix. The greatest concentrations were present near the bottom in the least turbid zones. In addition, concentrations greater than 200 particles per ml were present throughout the water column, yet no correlations were apparent when turbidity and distribution were compared. Observations by divers show that much of this material is churned from the bottom during periods of strong wave surge.

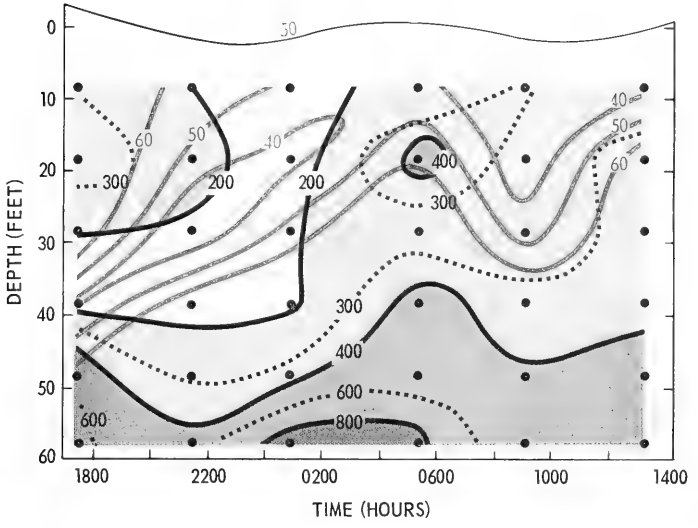

Figure 18. Distribution of total inanimate material (particles per ml), with transparency data (percent transmission) in red, Operation I.

TOTAL MICROCONSTITUENTS: Figure 19 represents the total of all microentities, animate and inanimate, enumerated in the study. The points of greatest concentration are positively correlated with the areas of greatest turbidity. The same positive correlation existed between total microorganisms and *Gymnodinium flavum*. This dinoflagellate represented 86 percent of total microorganisms and 65 percent of total microconstituents, and accordingly was the primary cause of light attenuation.

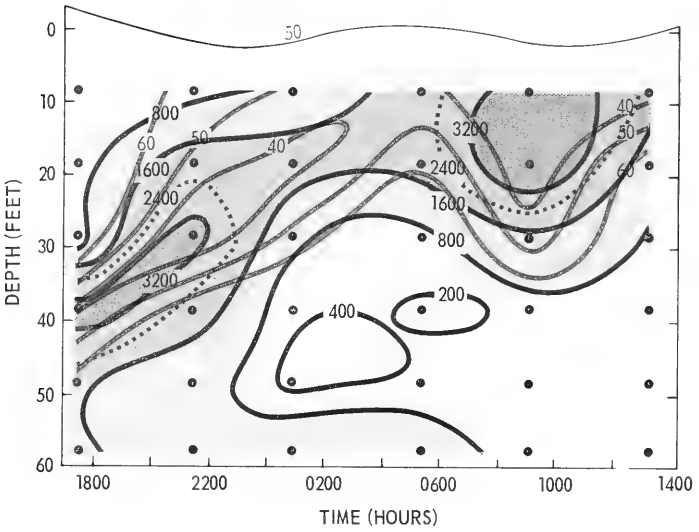

Figure 19. Distribution of total microconstituents (entities per ml), with transparency data (percent transmission) in red, Operation I.

TEMPERATURE AND THE DISTRIBUTION OF PARTICLES

Gymnodinium flavum: The 60-to-64°F isotherms (fig. 11) represented the area of most rapid thermal gradient and were used to delineate the thermocline. The distribution of *G. flavum* (fig. 12) corresponded closely in time and space with this thermal barrier. Figure 20 depicts the distribution of *G. flavum* with characteristic isotherms superimposed. Centers of highest population density were within the thermocline (1800 6 July at 38 feet) or above it (0900 7 July at 15 feet). Thus, a positive correlation existed not only between temperature and distribution but between transparency and distribution.

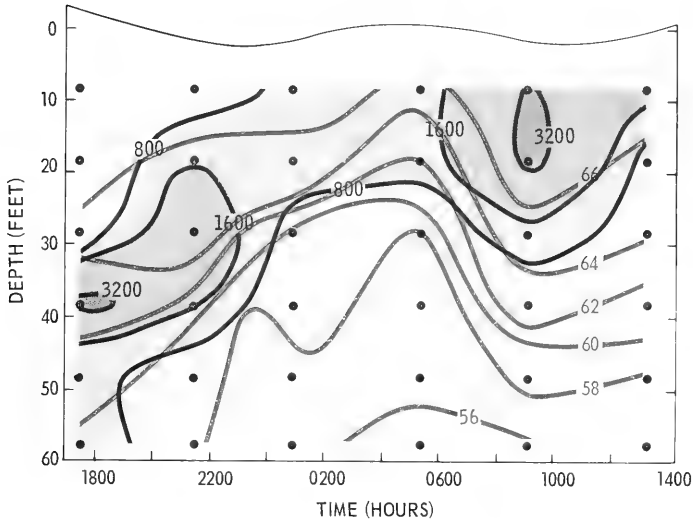

Figure 20. Distribution of *Gymnodinium flavum* with temperature in red, Operation I.

Ceratium fusus: The general distribution of *C. fusus* (fig. 13) corresponded with the thermocline in essentially the same fashion as the distribution of *G. flavum.* The areas of highest population were either within the thermocline (2100 6 July at 28 feet) or above it (0900 7 July at 8 feet).

Ceratium furca: Two centers of high population density (2100 6 July at 28 feet and 0900 7 July at 8 feet) (fig. 14) were distributed in and above the thermocline. A third was present below the thermocline at 1300 7 July at 48 feet. Between 1900 6 July and 0200 7 July the distribution penetrated the thermocline and extended to the bottom. These deviations from the distributional patterns demonstrated by *Gymnodinium flavum, C. fusus,* and other microorganisms may be attributable to concentrations of dead cells that have settled through the thermal barrier.

OTHER DINOFLAGELLATES: The several species of dinoflagellates (fig. 15) lumped here demonstrated the same general distribution as the preceding organisms. The bulk of the population was in or above the thermocline with the exception of a bottom extension between 2100 6 July and 0200 7 July.

DIATOMS: Present in low numbers (fig. 16), the vast majority of diatoms were distributed below the thermocline. This distribution is consistent with the conjecture that they were dead cells that had settled through the thermal barrier.

TOTAL MICROORGANISMS: As was true with the distribution of total cell counts and transparency, a positive correlation existed between total cell counts (fig. 17) and temperature gradients. The correlation was due to the presence of a thermal barrier and to the fact that 86 percent of the total microorganisms were represented by concentrations of *G. flavum,* which correlated with thermal structure. In addition, the cumulative contributions of *Ceratium fusus, C. furca,*

and other dinoflagellates, each of which correlated with the thermocline, strengthened the positive relationship between total microorganisms and temperature.

TOTAL INANIMATE MATERIAL: Inanimate material (fig. 18) was generally distributed throughout the water column and showed no obvious relation to thermal structure. Points of equal concentration are found within, above, and below the thermocline. Furthermore, the area of highest particle count (0100 to 0700 7 July) was found near the bottom, well below the thermocline, and represented material that had settled out of the water column or had been stirred up from the bottom by water movement.

TOTAL MICROCONSTITUENTS: With the exception of bottom concentrations from 1800 6 July to 0500 7 July, the distribution of all microconstituents (fig. 19) closely paralleled the thermal gradient and demonstrated the same general distributional pattern of the microorganisms that comprised the bulk of the particulate material in the water.

OPERATION II

TURBIDITY

A similar time-space graph of light transmission for Operation II is presented in figure 21. The light transmission ranged from 36 to 73 percent. The areas of greatest turbidity, with 50-percent light transmission or less, were present from near the sea floor to the surface around high tide between 1200 and 1700. This broad zone then narrowed. From 0400 through the remainder of the operation, the most turbid areas were confined to a relatively thin mid-water layer.

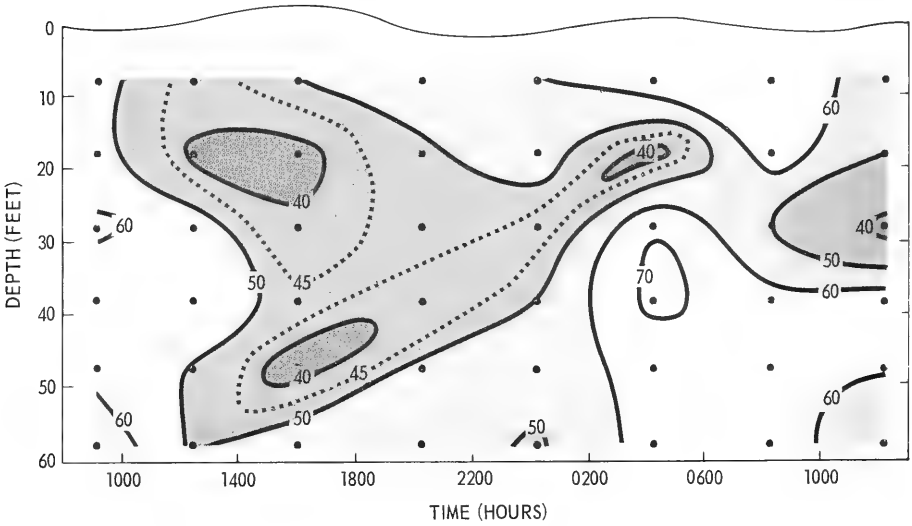

Figure 21. Water transparency (percent transmission), Operation II.

TEMPERATURE

The thermal regime (fig. 22) ranged from < 53°F at the bottom to > 71° at the surface. A relatively isothermal warm layer overlay an unusually strong thermocline. Within this region temperature generally decreased evenly from near the surface to the bottom. Two marked vertical oscillations were present. The crest of the first occurred between 1400 and 2200 20 July, and the second between 0200 and 1000 21 July. In each case the peak of the oscillation followed high tide (indicated at the surface) by approximately 2 hours.

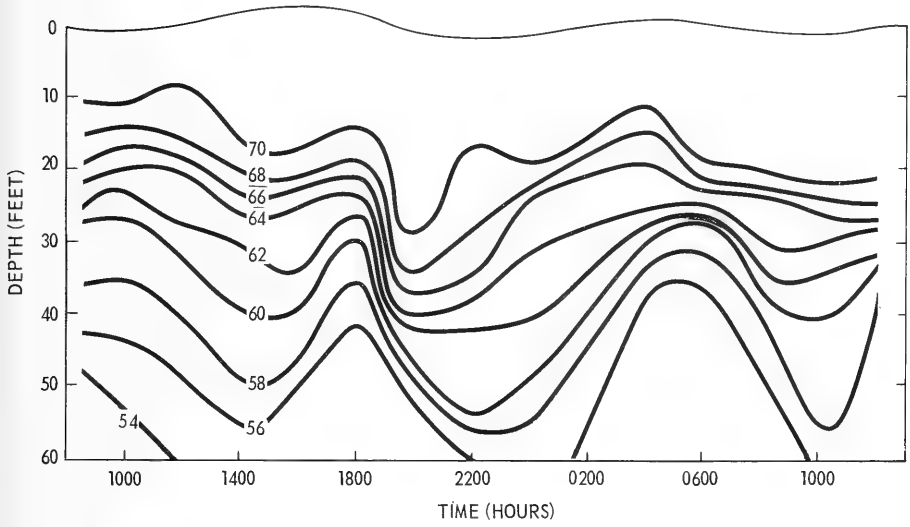

Figure 22. Water temperature (°F), Operation II.

Gymnodinium flavum: G. flavum (fig. 23) was present generally throughout the water mass. The highest cell counts fell predominantly within the turbid layer delineated by the 50-percent transmission contours (fig. 21). There were two exceptions -- a concentration between 2200 20 July and 0300 21 July from 50 to 32 feet, and another between 0600 and 1000 21 July at 48 feet. In both cases the maxima occurred in water 50 to 60 percent transparent and indicated that *G. flavum* alone was not responsible for the turbid pattern.

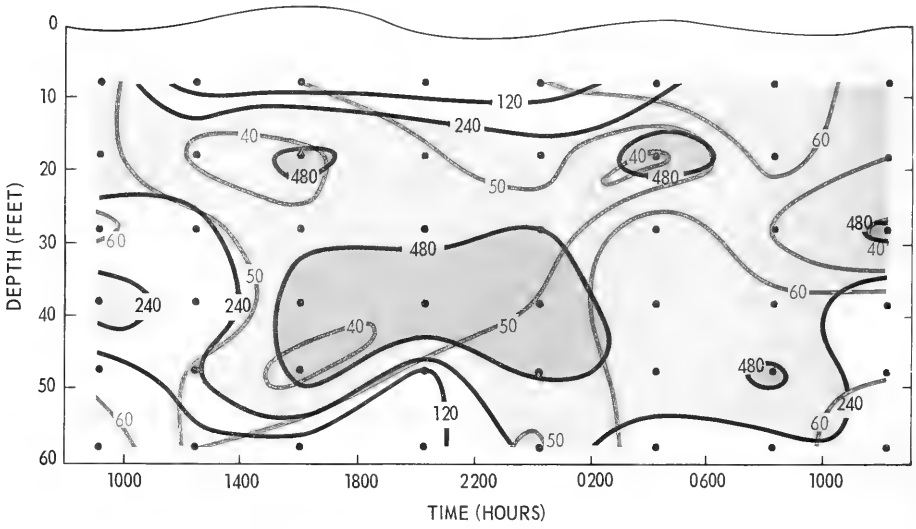

Figure 23. Distribution of *Gymnodinium flavum* (organisms per ml), with transparency data (percent transmission) in red, Operation II.

Ceratium fusus: Three areas of high population density (1300 at 8 feet, 1600 at 48 feet, and 0400 at 18 feet) (fig. 24) fell within or very close to the most turbid zones. A fourth concentration (2400 21 July at 38 feet) showed no relationship to light attenuation and emphasized that greater concentrations must be present before light transmission is significantly affected.

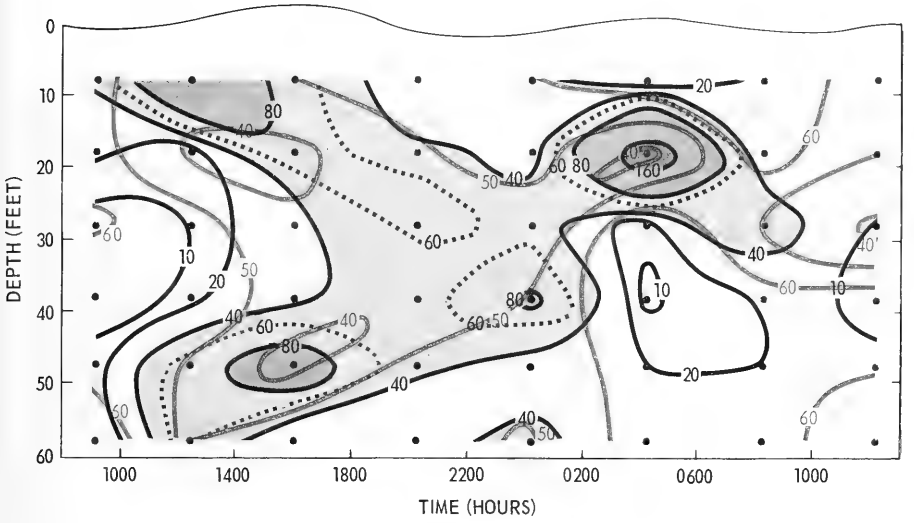

Figure 24. Distribution of *Ceratium fusus* (organisms per ml), with transparency data (percent transmission) in red, Operation II.

Ceratium furca: The distribution of *C. furca* (fig. 25) generally paralleled that of *C. fusus* and demonstrated the same relationship to turbidity. The low concentrations made it highly unlikely that *C. furca* contributed grossly to light attenuation. Rather, these concentrations were additive, turbidity being a function of a collection of particulate matter and dissolved substances rather than of any single organism.

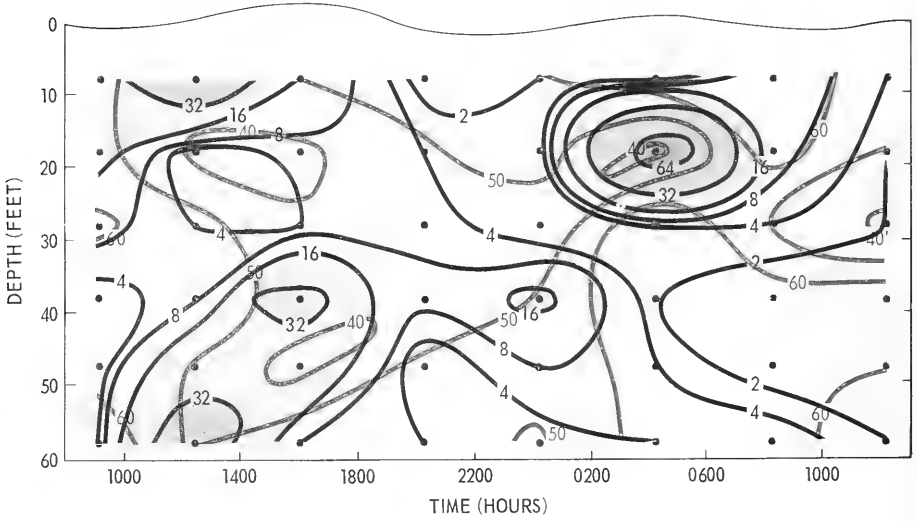

Figure 25. Distribution of *Ceratium furca* (organisms per ml), with transparency data (percent transmission) in red, Operation II.

OTHER DINOFLAGELLATES: The greatest concentrations of other dinoflagellates (fig. 26) appeared generally below 45 feet and were weaker than the concentrations of *Gymnodinium flavum* and *Ceratium fusus*. No clearly defined correlation existed between light transmission and the bulk of these organisms. A possible exception occurred at 0400 21 July, at 18 feet, where a concentration of organisms coincided in time and space with a turbid area.

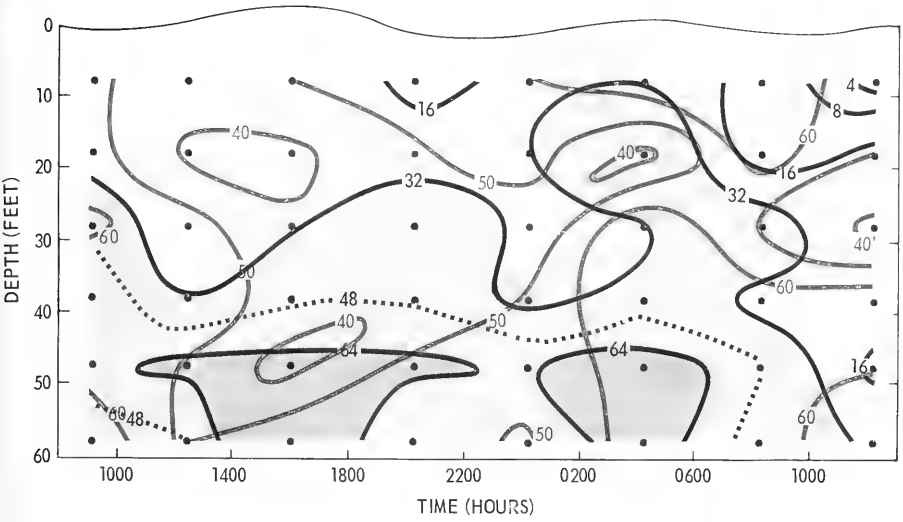

Figure 26. Distribution of other dinoflagellates (organisms per ml), with transparency data (percent transmission) in red, Operation II.

DIATOMS: Very low concentrations of diatoms (fig. 27) were present. Two points of highest concentration (1600 20 July at 48 feet and 1200 21 July at 28 feet) fall within the most turbid areas, but because of low cell counts this relationship was believed to be coincidental.

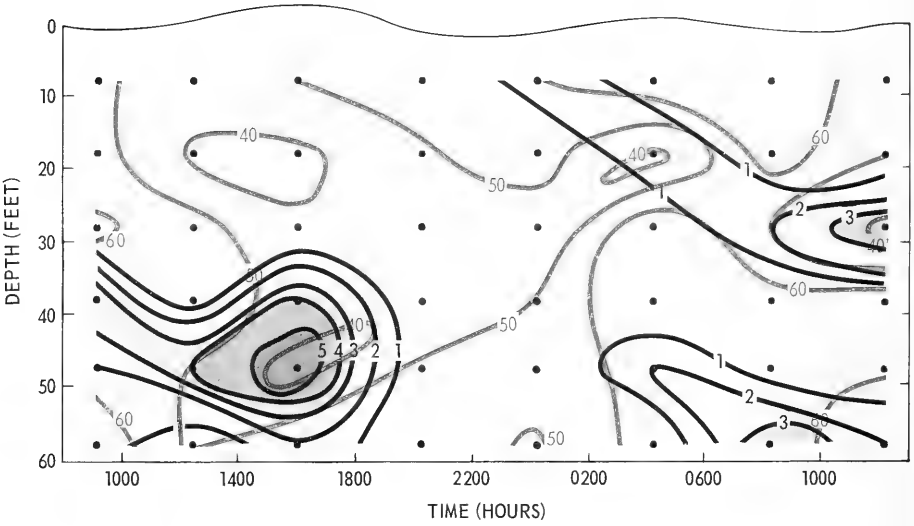

Figure 27. Distribution of miscellaneous diatoms (organisms per ml), with transparency data (percent transmission) in red, Operation II.

TOTAL MICROORGANISMS: The concentration of total microorganisms (fig. 28) ranged from 72 to 972 cells per ml. In general, concentrations above 400 cells per ml correlate positively with light attenuation. Doubts concerning a cause-and-effect relationship, however, are raised by a population greater than 400 cells per ml between 0200 and 1000 21 July at 48 feet. This concentration occurred in water which showed 60-percent light transmission and emphasizes the possible contribution of particles and dissolved substances not measured in this study. Furthermore, Operation I demonstrated that cells must be present in bloom quantities before they are major contributors to turbidity.

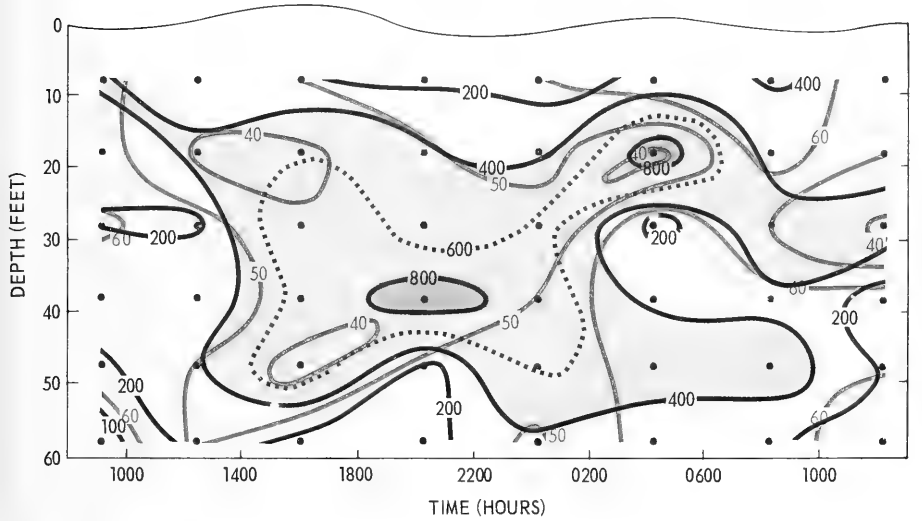

Figure 28. Distribution of total microorganisms (organisms per ml), with transparency data (percent transmission) in red, Operation II.

TOTAL INANIMATE MATERIAL: Isolated points in the distributional pattern of inanimate debris (fig. 29) correlated with the turbid layer. Additional points of high concentration, however, were found in water which showed light transmission above 60 percent. Such contradictions can be explained only on the basis of particles smaller than 10 microns and dissolved materials which were not measured in this study.

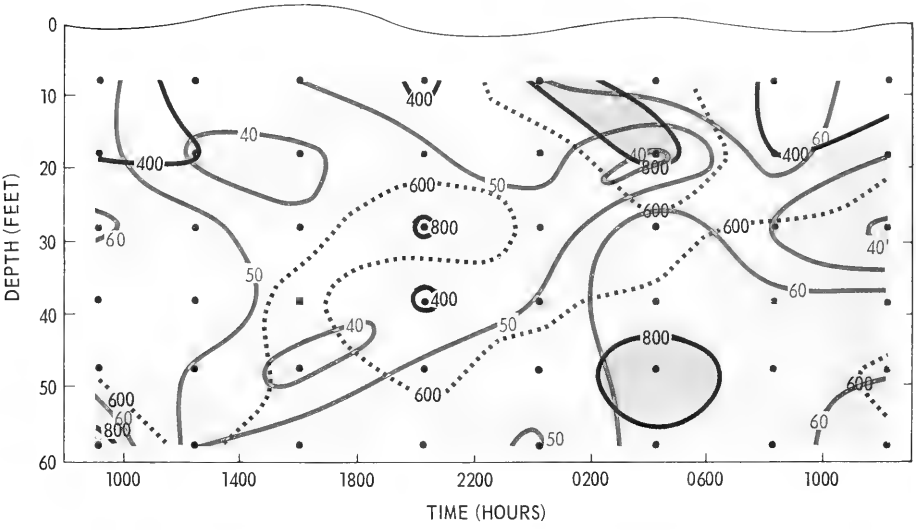

Figure 29. Distribution of total inanimate material (particles per ml), with transparency data (percent transmission) in red, Operation II.

TOTAL MICROCONSTITUENTS: The sum of all microentities counted is depicted in figure 30. With the exception of a concentration between 0200 and 1000 21 July at 48 feet, the distribution parallels turbidity.

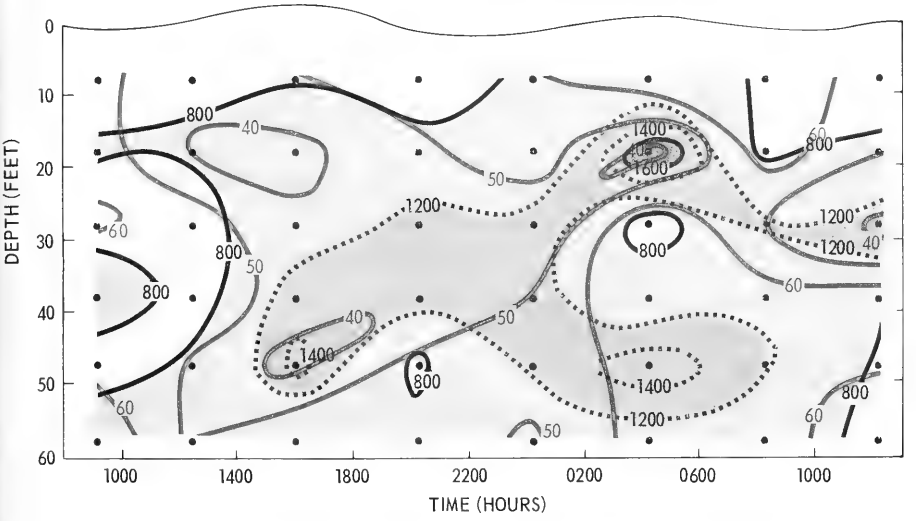

Figure 30. Distribution of total microconstituents (entities per ml), with transparency data (percent transmission) in red, Operation II.

Gymnodinium flavum: *G. flavum* was present (fig. 23) in relatively even concentration throughout the water column. Temperature (fig. 22) decreased markedly from 15 feet to the bottom, but the thermocline was broad and lacked the discrete thermal barrier present during Operation I. The organism appeared throughout the water mass, either as a function of the absence of a sharp thermal barrier, or as a function of bloom abatement.

Ceratium fusus: *C. fusus* (fig. 24) was distributed almost entirely below the 70°F isotherm which marked the top of the thermocline. The zone of highest population density (0400 21 July at 18 feet) correlated with a vertical oscillation in thermal structure.

Ceratium furca: The distribution of *C. furca* (fig. 25) followed the same pattern as that of *C. fusus*. The bulk of the population was found below the 70°F isotherm in water characterized by a constantly decreasing temperature gradient.

OTHER DINOFLAGELLATES: The several species lumped in figure 26 were largely distributed from 30 feet to the bottom and well below the 70°F isotherm. A population was present at 0400 21 July at 18 feet which corresponded to a vertical oscillation in the thermal structure.

DIATOMS: Very low concentrations of diatoms (fig. 27) were present and probably represented the frustules of dead cells. The concentrations showed no consistent relationship to temperature gradients.

TOTAL MICROORGANISMS: The time-depth distribution of all microorganisms (fig. 28) enumerated in this study parallels the distribution of *Gymnodinium flavum, Ceratium fusus,* and *C. furca.* With minor exceptions the cells are distributed below the 70°F isotherm. The points of highest population density (2000 20 July at 38 feet and 0500 21 July at 18 feet) were found to correlate with vertical oscillations in thermal structure.

TOTAL INANIMATE MATERIAL: The distribution of particulate material other than organisms (fig. 29) is general throughout the water column. Centers of highest concentration were found at the surface, in mid-water, and near the bottom. No general correlative pattern with temperature was apparent.

TOTAL MICROCONSTITUENTS: As expected, the distribution of total microconstituents (fig. 30) was similar to the distributions of the predominant individual microentities. The major areas of population density fell below the 70°F isotherm and were centered on the vertical oscillations of the thermal gradient cited previously.

RED WATER

While the occurrence of yellow-water blooms, noted in Operations I and II, is a rare event (Kofoid and Swezy, 1921,[17] Lackey and Clendenning, 1963[12]), recent years have seen a dramatic increase in the incidence of red-water outbreaks. The causal organism of this phenomenon in these waters is usually the small armored dinoflagellate *Gonyaulax polyedra*. Since 1959, during July and August, red water has been generally present in varying degrees off San Diego. Less frequent outbreaks occur during the fall and late spring months. Reduced water transparency at or near the surface off the southern California coast during warm weather months is primarily due to this phenomenon. Observations on red-water blooms from the NEL tower were conducted during the summer of 1964, and selected data pertinent to the prior work are included herein.

Transparency data acquired with the hydrophotometer were taken before, during, and after the passage of red-water patches through the tower site. Temperature was measured with a bathythermograph.

Figure 31 depicts light transmission and temperature during the passage of red water on 23 July 1964. On this date, the red water was first sighted seaward of the tower at 1010. By 1034, when the first hydrophotometer run was made, the red water was around the tower. A second and heavier concentration was observed approaching the tower at 1325. Light transmission on the descent of the hydrophotometer (fig. 32) at this time was 61 percent at the surface. Ascent, less than 10 minutes later through the center of this patch, showed surface transparency had been reduced to 38 percent, the difference undoubtedly attributable to the increase of *G. polyedra*. The passage of this red-water patch was bracketed by a hydrophotometer run at 1325 (fig. 31) and another at 1505, when the water began to clear. Transparency at the surface ranged from 31 to 89 percent between the hours of 1035 and 2100, when the last values were recorded. Variations in transparency from surface to near bottom through the same time period ranged from 31 to more than 90 percent.

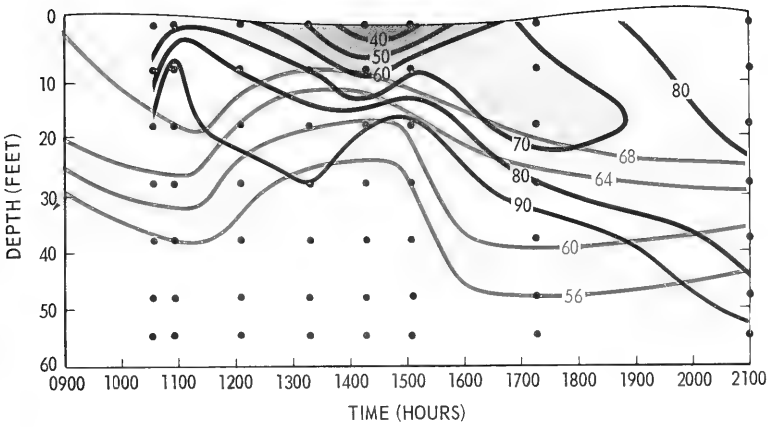

Figure 31. Water transparency (percent transmission), with temperature (°F) in red, 23 July 1964.

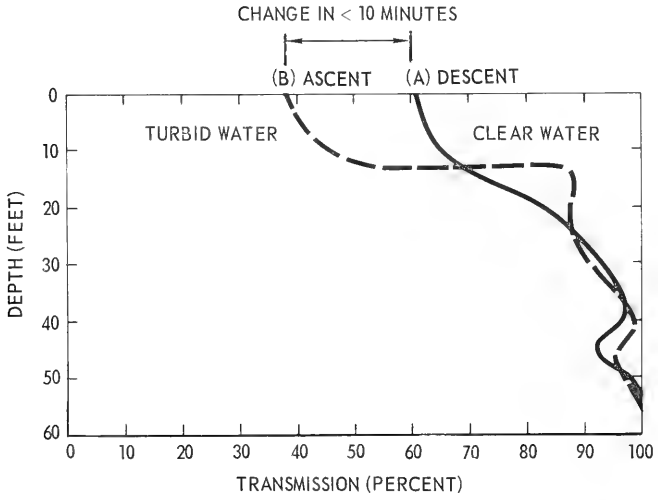

Figure 32. Hydrophotometer records on descent before maximum patch of red water arrived at the tower (A) and on ascent approximately 10 minutes later when patch of red water moved under the tower (B).

The thermal structure (fig. 31) on 23 July was characterized by a steep gradient and a pronounced vertical oscillation between the hours of 1056 and 1600. The oscillation produced a 15-foot upward displacement of the thermocline. Areas of least transparency (60 percent and less) are centered directly above the oscillation.

Figure 33 gives light transmission data for 24 July from 0030 to 1300. Transparency, measured at 0030 and 0515, was 75 percent or above throughout the water column. At 0905 turbid water appeared at 10 and 20 feet (53 and 58 percent, respectively), and at 1030 transparency between those depths (at 15 feet) had decreased to 45 percent. Surface transparency at 1030 was 70 percent. The first red water apparent at the surface appeared at the tower site at 1035. The hydrophotometer was operated at 1042 in the center of a large red-water mass. At this time, transmission ranged from 31 percent at the surface to more than 90 percent near the bottom. Light transmission increased from 47 percent at 20 feet to more than 90 percent at 30 feet. The red water persisted around the tower until after 1200. Extreme variation in transparency was measured during these operations. During the period from 0030 to 1300, transmission at the surface ranged from 31 to 87 percent. Surface to near-bottom values ranged from 31 to 99 percent.

In contrast to the situation on 23 July, temperature (fig. 34) between the hours of 0023 and 1133 on 24 July showed no major oscillations. The steepest gradient of the thermocline was between the surface and 40 feet with a range from 70°F at the surface to 54°F at 40 feet.

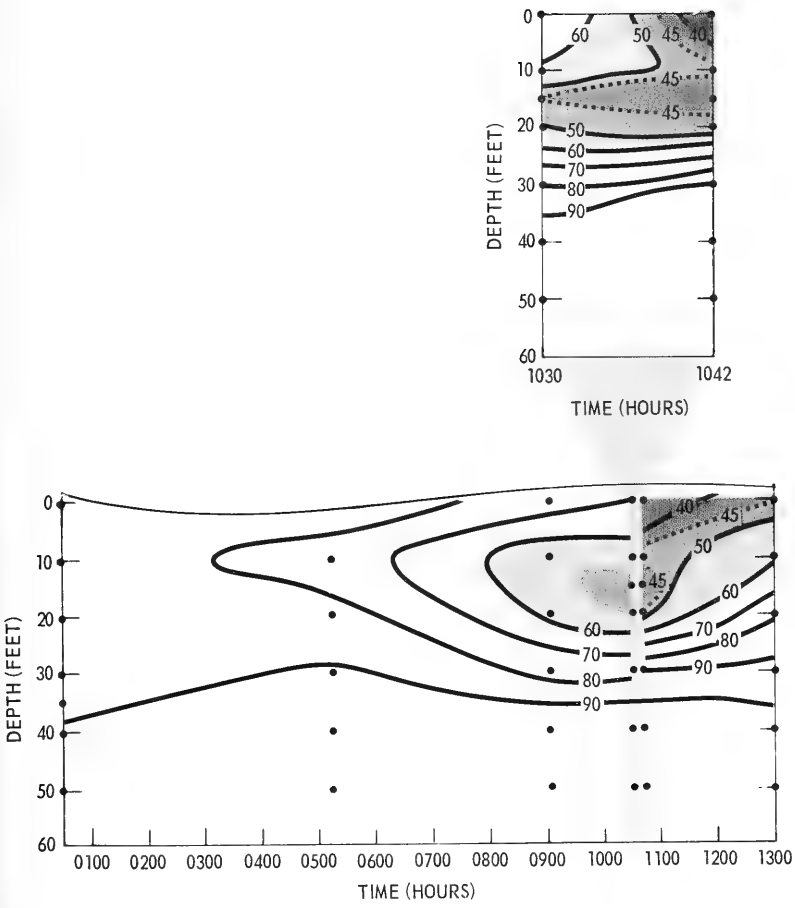

Figure 33. Water transparency (percent transmission) with one vertical run (1030) before the arrival of red water and a second run (1042) through red water surrounding the tower, 24 July 1964.

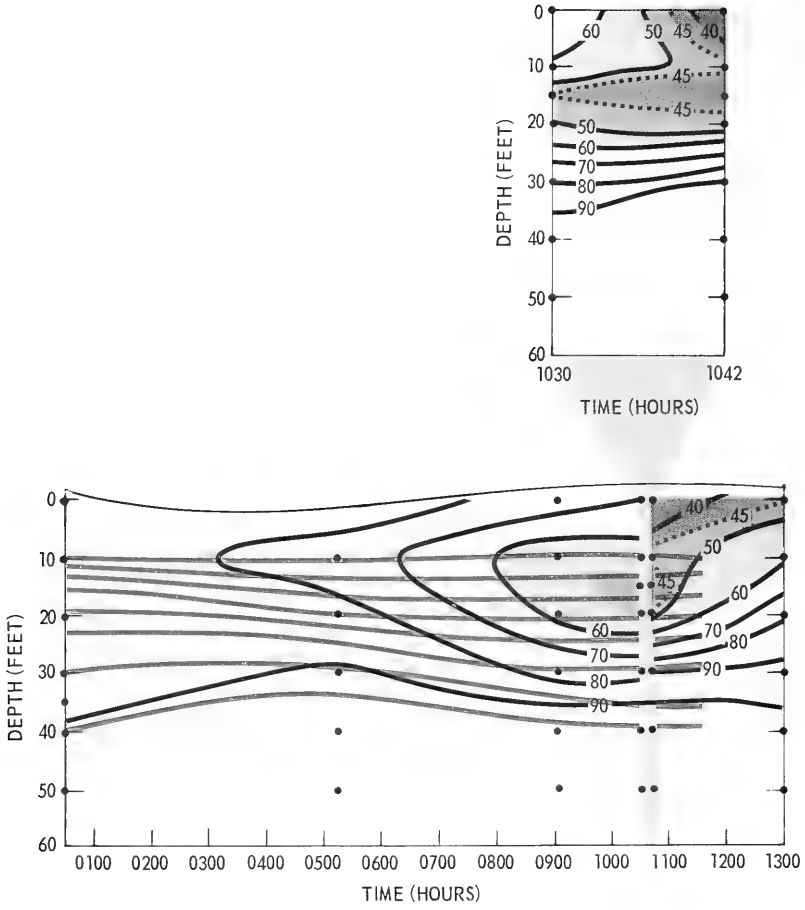

Figure 34. Water transparency (percent transmission), with temperature (^{o}F) in red, 24 July 1964.

DISCUSSION

The 2-week interval between Operations I and II permitted comparisons which emphasized the dynamic and complex nature of the environment. Physical data were compared to the distribution of organisms and correlations noted.

MICROCONSTITUENTS

OPERATION I

Operation I was conducted during a period of high concentration of *Gymnodinium flavum*. The organisms were distributed just above the thermocline and in it. Their level shifted as much as 40 feet in a few hours in accordance with the changing thermocline. Total microorganisms and total microconstituents showed the same pattern. An inverse relationship was demonstrated between light transmission and the distribution of *G. flavum*, total microorganisms, and total microconstituents. Specific points of population density in the distributional patterns of *Ceratium fusus*, *C. furca*, and other dinoflagellates compared positively to the distribution of total microorganisms and total microconstituents and indicated an additive contribution to turbidity.

The organisms cited were also distributed in or above the thermocline. This observation emphasized the role of thermal gradients in the distribution of organisms of this type.

The consistent and precise relationship between the distribution of *Gymnodinium flavum* and light transmission implicated it as a primary cause of turbidity. This observation was corroborated by correlations cited previously between the distribution of *G. flavum*, total microorganisms, and total microconstituents. The concentration of *G. flavum* reached 3.9×10^3 cells per ml and represented 65 percent of the total particulate material counted in this study.

While the degree of opacity and the true distribution of these cells are unknown, calculations relating the combined surface area of *G. flavum* at this high concentration to the cross-sectional area of the light path (refer to MATHEMATICAL TREATMENT) indicated that cells in the quantity sampled are sufficient to account for the measured turbidity. Furthermore, examination of least-squares lines (figs. 8A and C) and the theoretical curves (figs. 9A and C) reveals positive correlations between concentrations of *G. flavum* and total microconstituents compared to light transmission, particularly when particle counts exceed 10^3 per ml.

The correlation between the distribution of microorganisms and the thermocline is suggestive of two possibilities -- the colder water of the thermocline served as a density barrier on which microorganisms settled and the increased density concentrated organic debris necessary to the microorganisms. Sorokin (1960)[11] cites the possibility of more intensive multiplication of cells in the nutrient-rich layer of the thermocline. He further cites thermal density stratification as one of the main factors determining the vertical distribution of phytoplankton. Using underwater television and scuba at the tower site, the authors have frequently observed the increased turbidity associated with the thermocline.

Diatoms, fecal pellets, wood fibers, and miscellaneous debris (refer to appendix) showed no discernible relationship to turbidity except as these populations may have contributed to bottom concentrations shown in total microconstituents.

OPERATION II

Operation II was characterized by an essentially constant temperature gradient, a more diffused distribution of the predominant microorganism *Gymnodinium flavum,* fewer cells, and a different turbidity pattern.

The examination of distribution charts and transparency data revealed no consistent patterns or positive correlations. Least-squares data (figs. 8B and D) and the theoretical curves (figs. 9B and D) supported the conclusion that the concentrations of *G. flavum* cells and total microconstituents were too low to affect transparency in the manner demonstrated in Operation I. Thus, no single microorganism appeared to be a major contributor to light attenuation. Rather, turbidity at this time was the result of a background concentration of *G. flavum* distributed throughout the water mass, a collective distribution of other particulate matter, and, very probably, dissolved organic material. *Ceratium furca* and *C. fusus* contributed to specific zones of population density in the distribution of total microorganisms. The distribution of other dinoflagellates, diatoms, fecal pellets, wood fibers, and miscellaneous detritus was not shown to be related to the turbidity patterns.

Undoubtedly, particles less than 10 microns in diameter, pigments released from decomposing cells, and dissolved organic material, none of which were measured in this study, played a significant role in light absorption and scatter at this time. For example, Burt (1955)[6] notes that a large share of the particles causing extinction have a radius of less than one micron.

The contrast between the distribution of *G. flavum* during the two operations emphasized the role of temperature gradients. The presence of a sharp thermocline during a bloom of *G. flavum* (Operation I) produced a definite correlation between temperature and cell distribution in time and space. The more general distribution of *G. flavum* in Operation II is believed to have resulted from the absence of a discrete thermal barrier.

The effect of thermal barriers on phytoplankton distribution may also be a function of timing with respect to bloom period. Provided the rate of cell division at the

onset of a bloom is logarithmic, the period of time corresponding to this portion of the growth curve would produce a preponderance of living cells with optimal motile capacities. As limiting environmental factors became critical, the rate of cell division would decline and mortality would rise. The number of dead cells would increase, and the dead cells would slowly sink, at a declining rate, as the water density increased. Operation II, with an even temperature gradient, provides a theoretical situation in which the distribution of phytoplankton was a function of bloom decline as well as of temperature. Tables 1 and 2 sum up pertinent data for each microorganism.

MACROPLANKTON

The distribution charts of macroplankton (refer to appendix) were compared to the temperature structure and turbidity. The only positive relationship demonstrated was with volume displacement, Operation I (fig. 35). The correlation was not supported by the individual counts of macroplankton and was caused by reduction of the effective mesh size of the net by clogging, so that much of the finer material (that is, *Gymnodinium flavum*) was retained and dominated volume displacement.

The large relative size and low concentrations of macroplankton made negligible their contribution to total biomass and the attenuation of light.

In certain cases at night swarms of mysids are attracted to the light beam of the hydrophotometer and can greatly affect light transmission. High numbers of copepod nauplii in a freshwater lake were also shown to affect transparency.

The distributional patterns of macroorganisms for both operations were also compared. No consistent relationships were apparent with respect to vertical distribution, diurnal migration, or tidal activity.

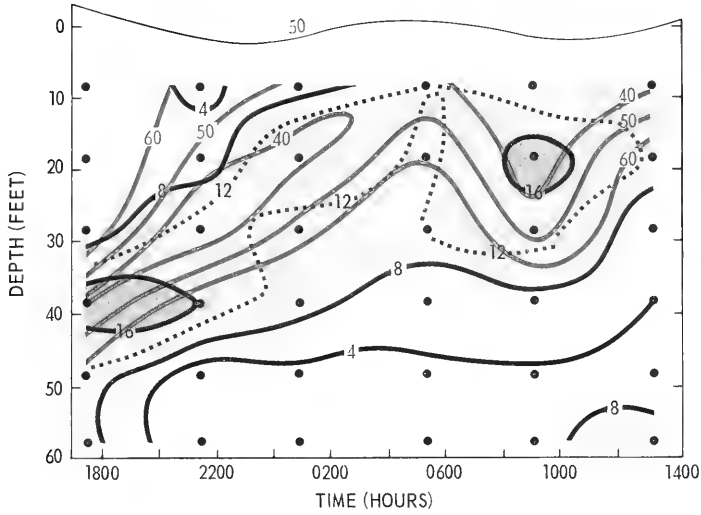

Figure 35. Fractional volume displacement (filtered material times 10^{-3} liters), with transparency data (percent transmission) in red, Operation I.

RED WATER

The presence of intense concentrations of red water caused by *Gonyaulax polyedra* during daylight hours 23, 24 July 1964 made possible the correlation of visual observations from the NEL tower and from scuba-equipped divers in the water. The observations, coupled with temperature data, substantiated the data taken in 1961.

The zone of greatest turbidity on 23 July (fig. 31) was centered directly above the long-period vertical oscillation of the thermocline cited previously. The lowest

light transmission (31 percent) recorded during the period closely approximated the high point of the oscillation. This long-period disturbance was believed responsible for the appearance of *G. polyedra* at the surface and indicates again the role played by thermal density stratification in the distribution of microorganisms. Scuba observers estimated underwater visibility to be 5 feet in the most turbid area. Visibility increased to 20 feet at a depth of 15 feet. Deeper water showed visibility of approximately 40 feet. These observations correlated closely with hydrophotometer data. The passage of this red-water patch was observed from the bottom by a diver who likened its approach to that of a line squall. While near-bottom water was clear, diver activity under a front of this type would be hampered by the reduction in light from the surface.

Figure 32 illustrates the rapid change in transparency during the passage of red water. It is believed that the 23-percent reduction in transparency was caused entirely by the passage of red water.

On 24 July the transparency and temperature data (figs. 33 and 34) suggest a large patch of red water, at subsurface depths, which reached the measurement site at approximately 0905. This conjecture is consistent with the presence of a thicker thermocline and therefore a more gently sloping density barrier within which the organisms would be dispersed more evenly. The presence of red water below the surface is commonly revealed in the wake of a ship when the organisms are churned to the surface by the propeller. The surface red water around the tower at 1042 (fig. 33) probably represented a short-term divergence not apparent when temperature was taken at relatively long intervals.

THERMAL-STRUCTURE CYCLES

Of interest were the various time cycles in the depth of the thermocline. Considerable study has been made of the short-period vertical oscillations in the thermocline caused by internal waves. Internal waves are instrumental in changing the level of the thermocline as much as 30 feet in a few minutes. In addition, it is known that the thermocline fluctuates with the tide but not necessarily in phase with it. There is, however, a diurnal movement of surface water onshore and offshore in accordance with the diurnal wind system. The WNW component of the usual daily sea breeze, in accordance with the Ekman effect, lowers the thermocline at the tower. This component reaches its maximum in the early evening and terminates at night. The night termination, with an occasional weak reversal, creates an offshore displacement and a rise in thermocline with a minimum depth early in the morning. Thus, sampling every 4 hours allows the longer periods of thermocline oscillation to be considered, even though they are greatly influenced by short-period internal waves (Cairns and LaFond, 1965).[18]

SUMMARY AND CONCLUSIONS

The main portion of the study was conducted through two time periods in July 1961. Particles greater than 10 microns (to a maximum of 2 mm), both animate and inanimate, were enumerated. The organisms were separated into microorganisms and macroorganisms. The distribution of all entities in time and space was compared to temperature and light transmission and causal relations were established.

Two different situations, 2 weeks apart, have been discussed. The obvious differences were in light transmission, temperature, and distributional patterns of organisms.

Additional data taken during a red-water bloom July 1964 were included.

Operation I was conducted during a yellow-water bloom of *Gymnodinium flavum.* A thermocline was present which correlated with turbidity and the distributional pattern of *G. flavum,* total microorganisms, and total microconstituents. The concentration of *G. flavum* represented 65 percent of the total particulate count, and it was this high concentration which apparently contributed most to turbidity and produced the correlation between total microorganisms and total microconstituents.

Other microentities demonstrated additive contributions to the turbidity pattern.

The distribution of *G. flavum* on the thermocline was thought to result from increased water density or a concentration of nutrients in the denser water attractive to these organisms.

Operation II was characterized by a relatively constant temperature gradient, a more general turbid pattern, and a corresponding lack of high correlation between any one microorganism, temperature, and turbidity. Light attenuation was the result of a diffused background concentration of *G. flavum* and a collective distribution of other particulate matter. Particles less than 10 microns, pigments, and bacteria, not measured here, undoubtedly played an important role in light attenuation.

The more general distribution of *G. flavum* was attributable to the absence of pronounced thermal stratification and the stage of the bloom cycle. The operation came near the end of the bloom with the probability of a higher incidence of dead or inactive cells which were affected to a greater degree by variation in water movement and density.

The contribution of macroplankton, present in relatively low numbers, to light attenuation was not apparent in either operation.

Data taken during the presence of red water in July 1964 supported the conclusions that single-celled organisms in bloom quantities seriously affect light transmission, and the distribution of these organisms is affected by thermal gradients.

An extensive literature documents the complexity of causal factors on transparency in the sea. These works clearly demonstrate the difficulties of attempting to generalize from a limited study. The wide range of organisms, materials, and other factors which are cited as reducing light transmission includes not only concentrations of organisms but their size, morphological variation, optical density, pigmentation, metabolic products, and decomposition products, including released pigment. Further, a vast spectrum of other light-intercepting debris, both organic and inorganic, must be considered. To this imposing array of entities are added the vagaries of physical factors such as tide, temperature, current, and salinity. For example, it has recently been shown that the formation of organic aggregates (Sutcliffe *et al*, 1963)[19] is associated with the adsorption of material on bubbles. Presumably, air churned into the water by breaking waves would produce bubbles in the sea. Oxygen-saturated water, such as exists at times of bloom, would tend to create bubbles more readily. Thus, such factors as the state of the sea and oxygen content of the water must also be considered.

The development of the ability to predict turbidity will demand an understanding of all the aforementioned, and is beyond the scope of this study.

RECOMMENDATIONS

The values of turbidity and their related abundance of organisms should be used when optical or visual operations or installations are required.

The relation of phytoplankton blooms to physical and chemical phenomena should be studied to produce criteria enabling prediction of plankton bloom development and abatement.

The effect of phytoplankton blooms on sound transmission should be investigated.

Diver vision should be correlated with hydrophotometer measurements and biological populations. The effects of various biological populations on the operation of underwater lasers should be investigated. Bioluminescence should be measured and correlated with concentrations of dinoflagellates and water transparency.

Size, origin, and geographic distribution of colored water masses should be observed from airplanes and satellites. The relation between light transmission and seasonal blooms of phytoplankton should be established.

REFERENCES

1. Holmes, R. W., "Solar Radiation, Submarine Daylight, and Photosynthesis," Geological Society of America Memoir 67, v.1, p.109-128, 1957

2. Tyler, J. E. and Preisendorfer, R. D., "Transmission of Energy Within the Sea: Light," p.397-451 in The Sea, v.1, edited by M. N. Hill, Interscience, 1962

3. Parsons, T. R., "Suspended Organic Matter in Sea Water," p.205-239 in Progress in Oceanography, v.1, MacMillan Company, 1963

4. Hart, T. J., "Notes of the Relation Between Transparency and Plankton Content of the Surface Waters of the Southern Ocean," Deep-Sea Research, v.9, p.109-114, 1962

5. Young, Jr., R. T., "Measurements on the Transparency of Sea-Water Off the Coast of Southern California," Journal of Marine Research, v.2, p.117-125, 1939

6. Burt, W. V., "Distribution of Suspended Materials in Chesapeake Bay," Journal of Marine Research, v.14, p.47-62, 1955

7. LaFond, E. C. and Sastry, J. S., "Turbidity of Waters Off the East Coast of India," Indian Journal of Meteorology and Geophysics, v.8, p.183-192, April 1957

8. Ball, T. F. and LaFond, E. C., "Turbidity of Water Off Mission Beach," p.37-44 in Pacific Science Congress, 10th, Honolulu, 1961. Physical Aspects of Light in the Sea; a Symposium, J. E. Tyler, editor, Honolulu, University of Hawaii Press, 1964

9. Gessner, F., "The Vertical Distribution of Phytoplankton and the Thermocline," Ecology, v.29, p.386-389, 1948

References (Continued)

10. Johnson, M. W., "Relation of Plankton to Hydrographic Conditions in Sweetwater Lake," American Water Works Association. Journal, v. 41, p. 347-356, April 1949

11. Sorokin, J. I., "Vertical Distribution of Phytoplankton and the Primary Organic Production in the Sea," Journal du Conseil (International Council for the Study of the Sea), v. 26, p. 49-56, 1960

12. Lackey, J. B. and Clendenning, K. A., "A Possible Fish-Killing Yellow Tide in California Waters," Florida Academy of Sciences. Quarterly Journal, v. 26, p. 263-268, 1963

13. LaFond, E. C., "How It Works - The NEL Oceanographic Tower," U. S. Naval Institute. Proceedings, v. 85, p. 146-148, November 1959

14. U. S. Fish and Wildlife Service Special Scientific Report Fisheries 433, The Preparation of Marine Phytoplankton for Microscopic Examination and Enumeration on Molecular Filters, by R. W. Holmes, June 1962

15. Richards, F. A. and Thompson, T. G., "The Estimation and Characterization of Plankton Populations by Pigment Analyses. II. A Spectrophotometric Method for the Estimation of Plankton Pigments," Journal of Marine Research, v. 11, p. 156-172, 1952

16. Banse, K. and others, "A Gravimetric Method for Determining Suspended Matter in Sea Water Using Millipore Filters," Deep-Sea Research, v. 10, p. 639-642, 1963

17. Kofoid, C. A. and Swezy, O., "The Free-Living Unarmored Dinoflagellata," California. University. Memoirs, v. 5, p. 45, 1921

References (Continued)

18. Cairns, J. L. and LaFond, E. C., "Prediction of Summer Thermocline Depth Off Mission Beach," p. 111-132 in Naval Ordnance Laboratory, Second United States Navy Symposium on Military Oceanography, 5-7 May 1965. The Proceedings of the Symposium, vol. 1, 1965

19. Sutcliffe, Jr., W. H. and others, "Sea Surface Chemistry and Langmuir Circulation," Deep-Sea Research, v. 10, p. 233-243, 1963

APPENDIX: TIME-DEPTH CHARTS

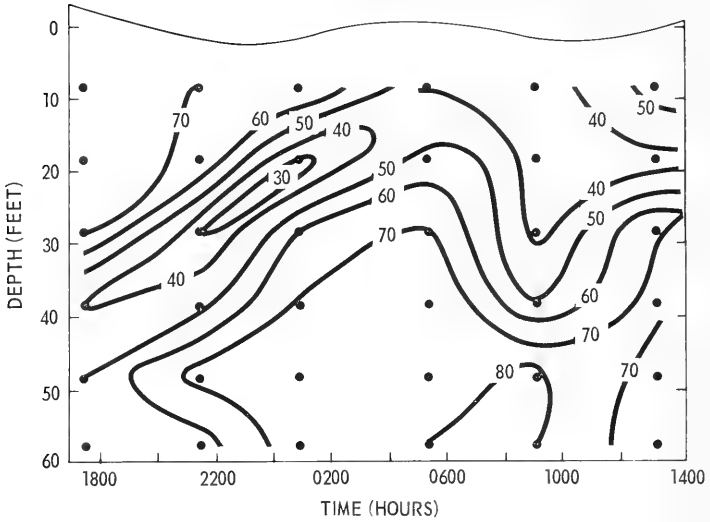

Figure A1. Water transparency (percent transmission) taken at the time of macroplankton runs, Operation I.

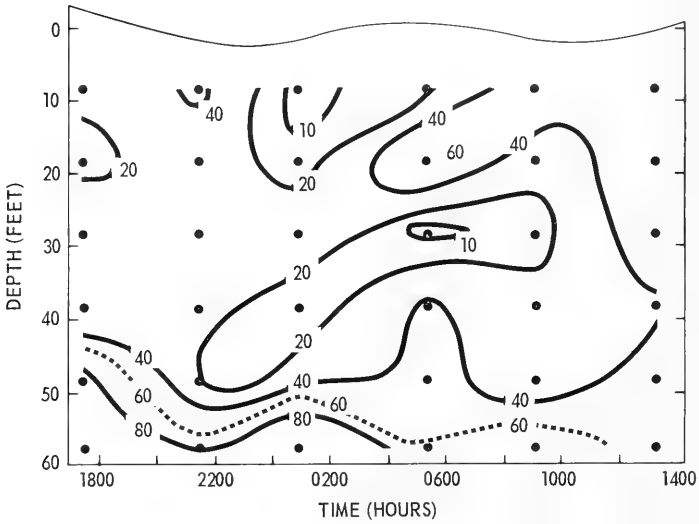

Figure A2. Distribution of organic aggregates (particles per ml), Operation I.

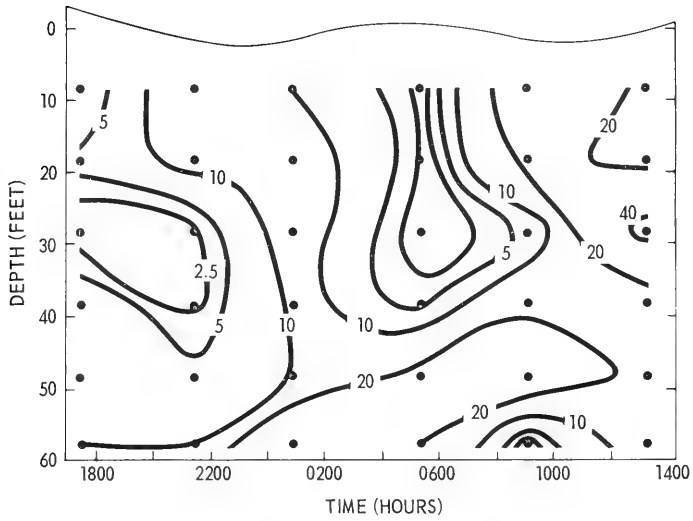

Figure A3. Distribution of wood fibers (particles per ml), Operation I.

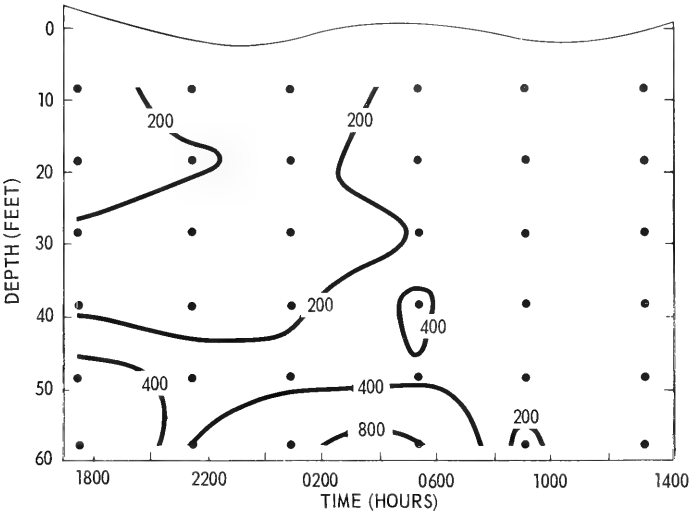

Figure A4. Distribution of unidentified particles (particles per ml), Operation I.

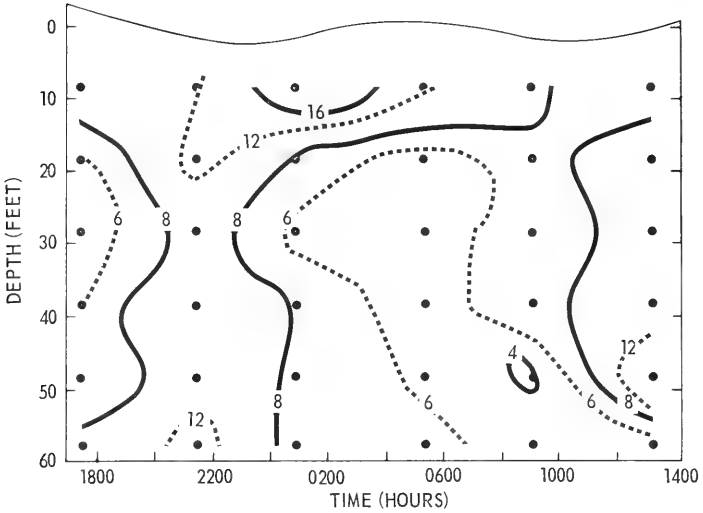

Figure A5. Distribution of copepods (organisms per liter), Operation I.

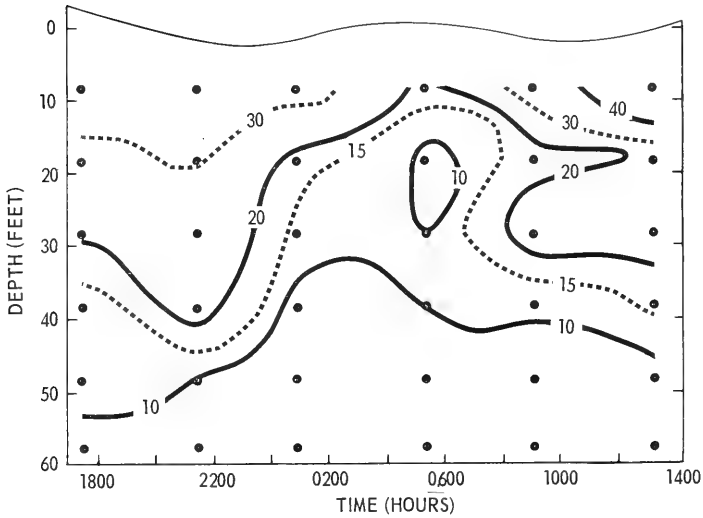

Figure A6. Distribution of nauplii (larvae) (organisms per liter), Operation I.

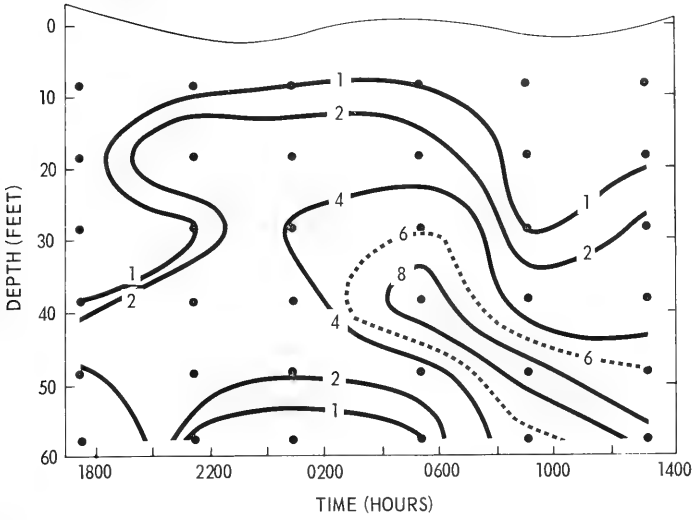

Figure A7. Distribution of polychaete larvae (organisms per liter), Operation I.

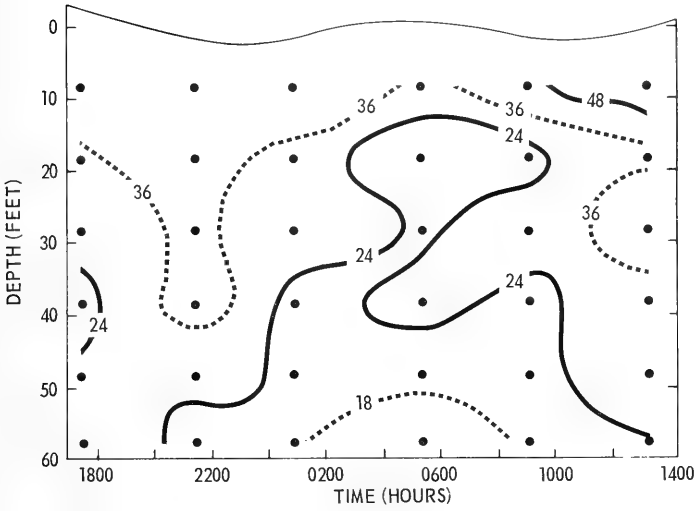

Figure A8. Distribution of total macroplankton (organisms per liter), Operation I.

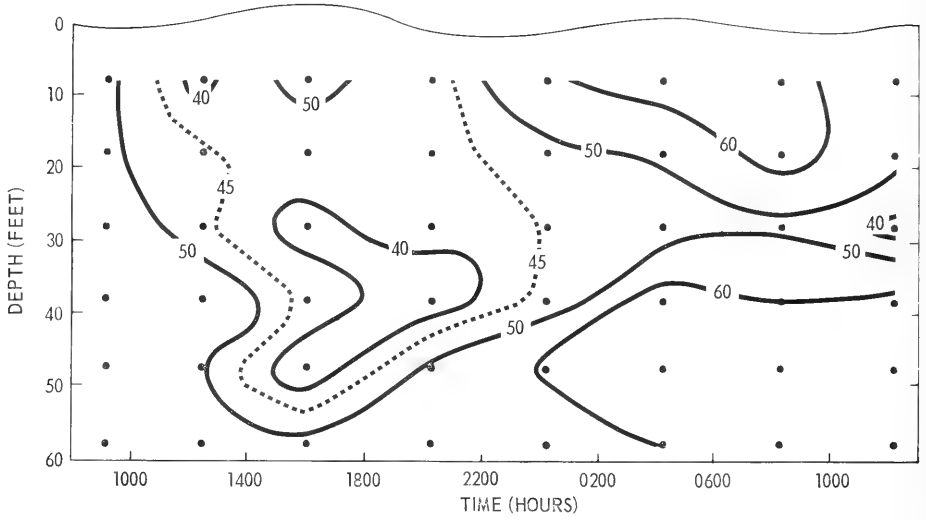

Figure A9. Water transparency (percent transmission) taken at the time of macroplankton runs, Operation II.

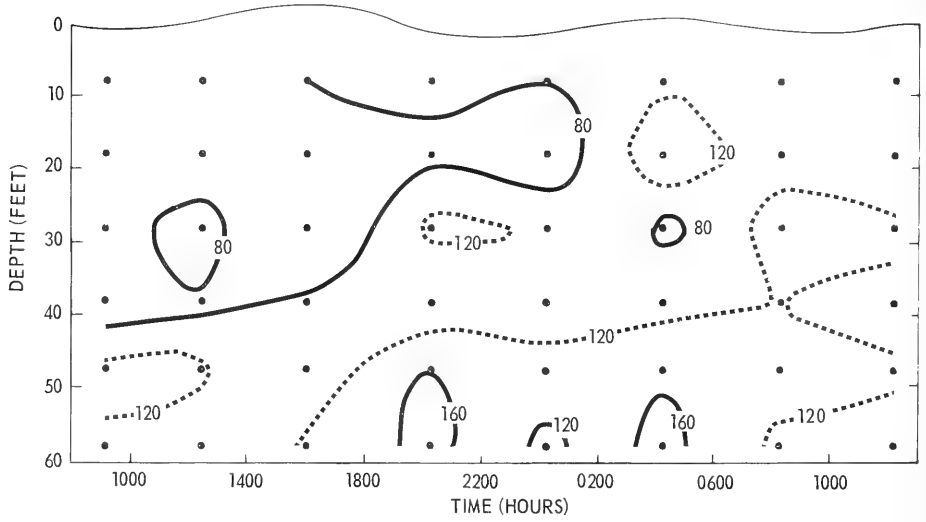

Figure A10. Distribution of organic aggregates (particles per ml), Operation II.

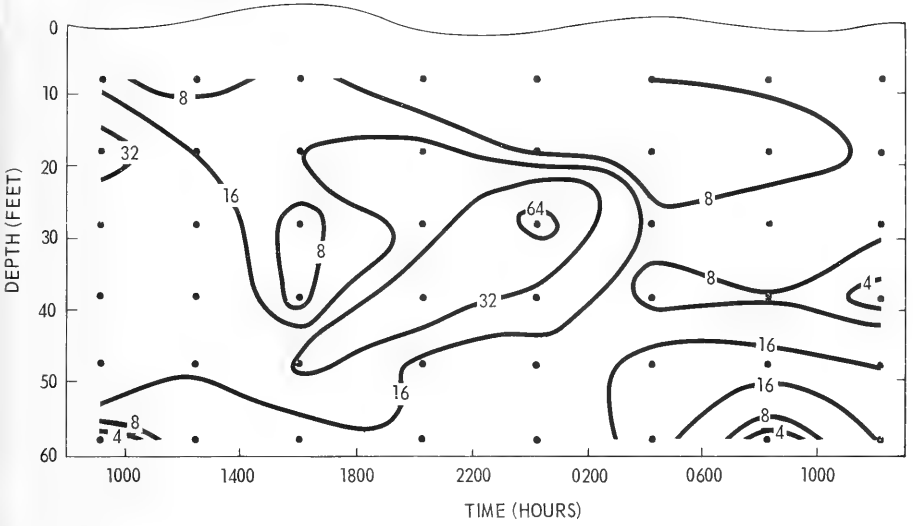

Figure A11. Distribution of wood fibers (particles per ml), Operation II.

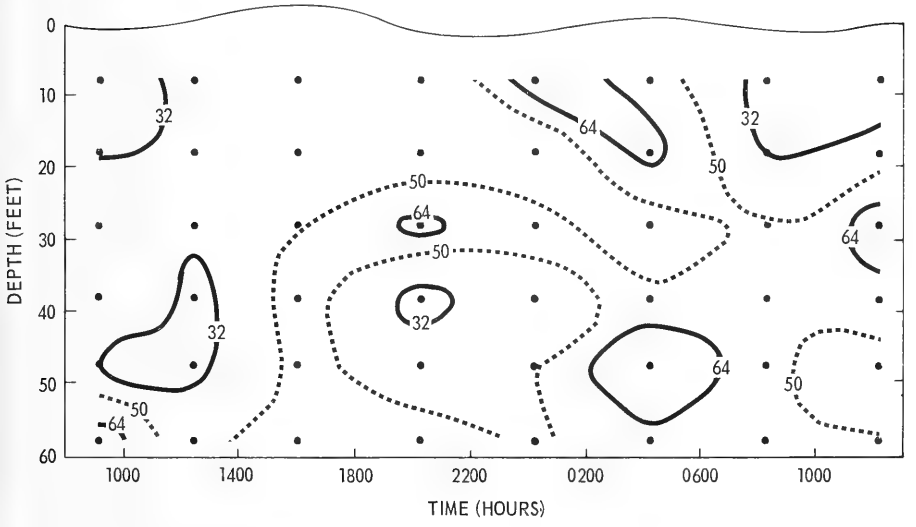

Figure A12. Distribution of unidentified particles (particles per ml), Operation II.

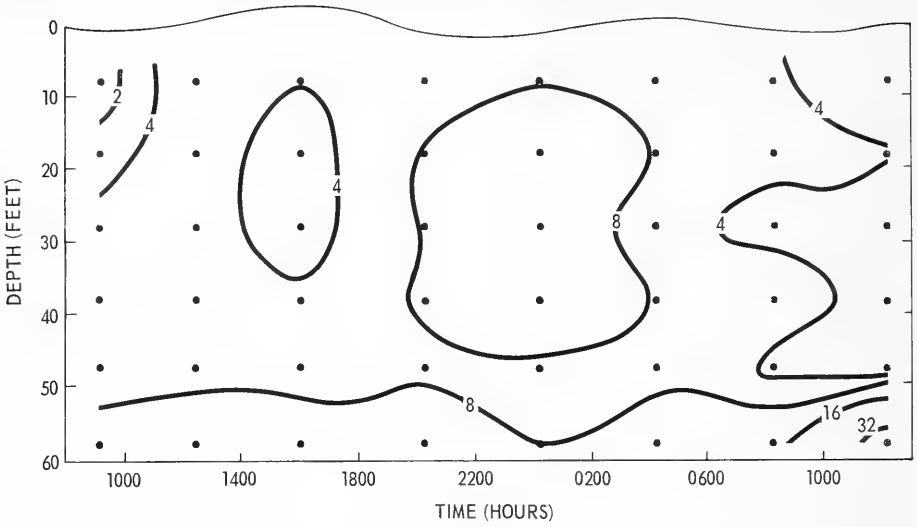

Figure A13. Distribution of copepods (organisms per liter), Operation II.

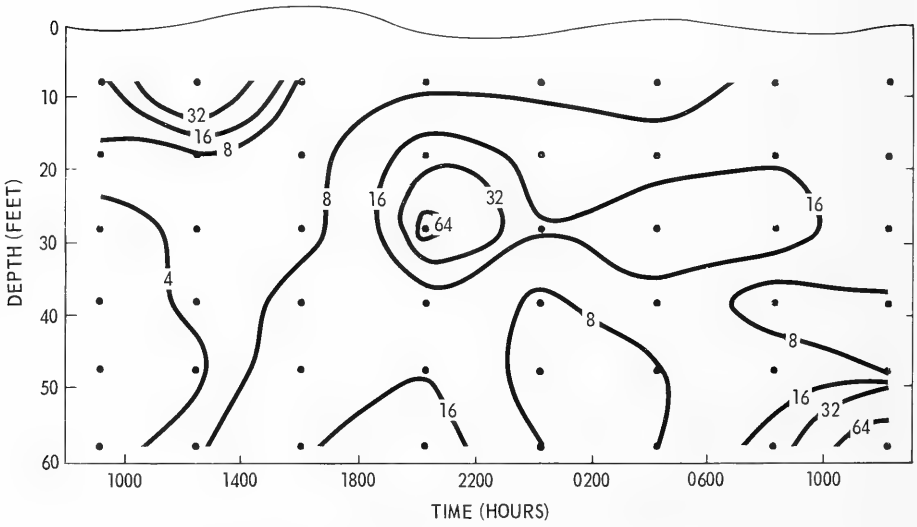

Figure A14. Distribution of nauplii (larvae) (organisms per liter), Operation II.

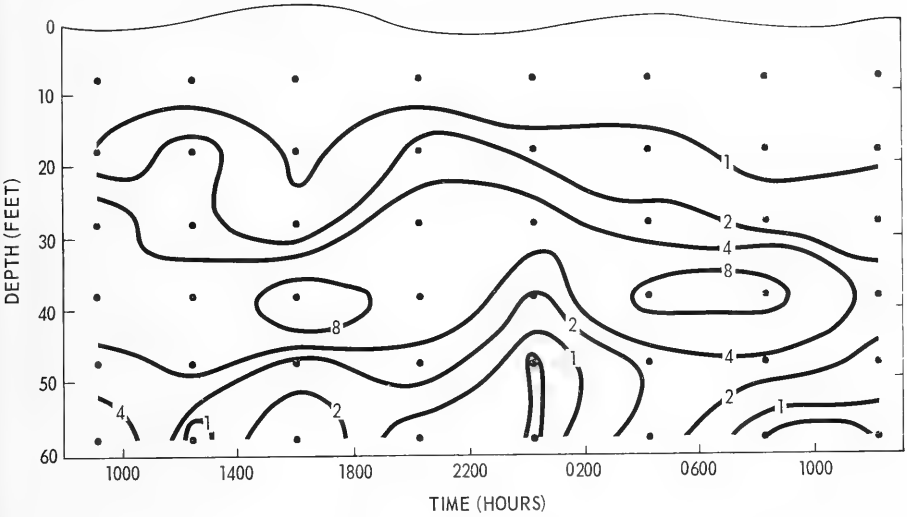

Figure A15. Distribution of polychaete larvae (organisms per liter), Operation II.

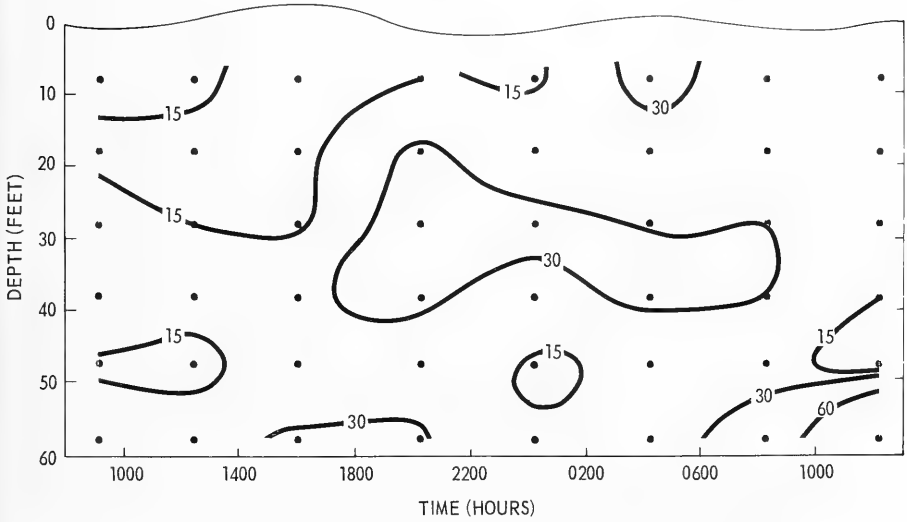

Figure A16. Distribution of total macroplankton (organisms per liter), Operation II.

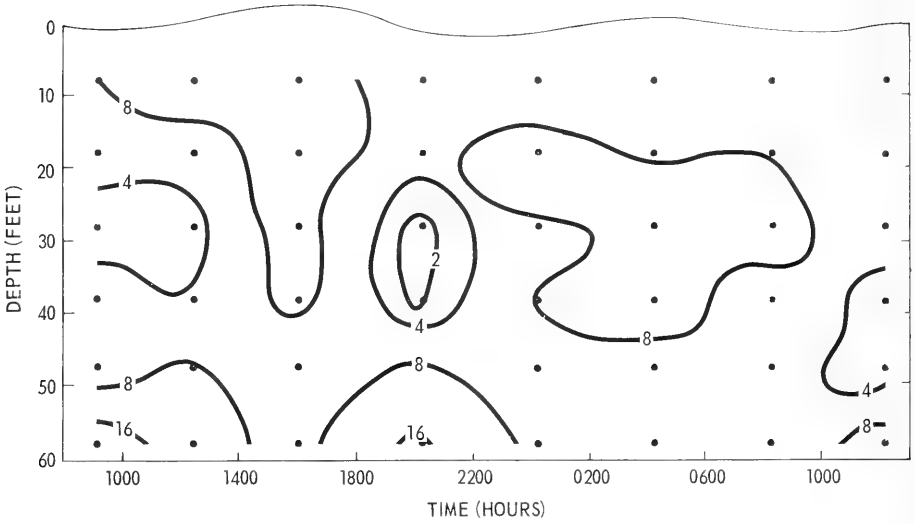

Figure A17. Volume displacement (filtered material), Operation II.

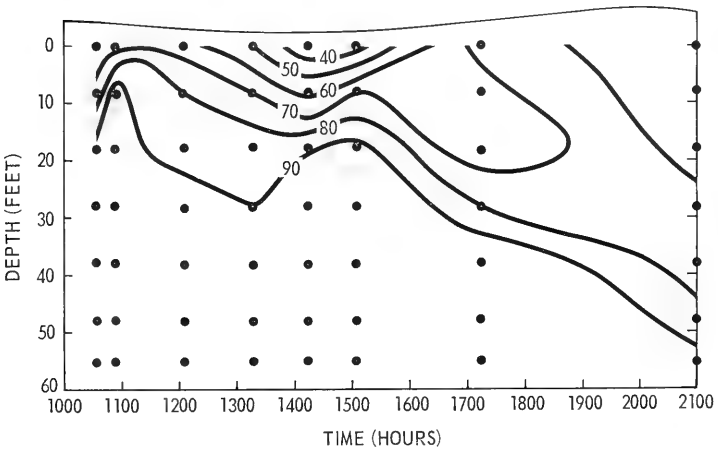

Figure A18. Water transparency (percent transmission) 23 July 1964.

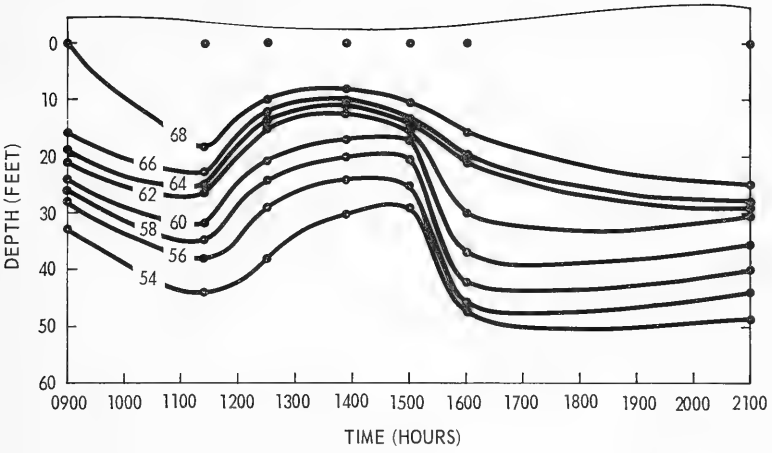

Figure A19. Water temperature (°F) 23 July 1964.

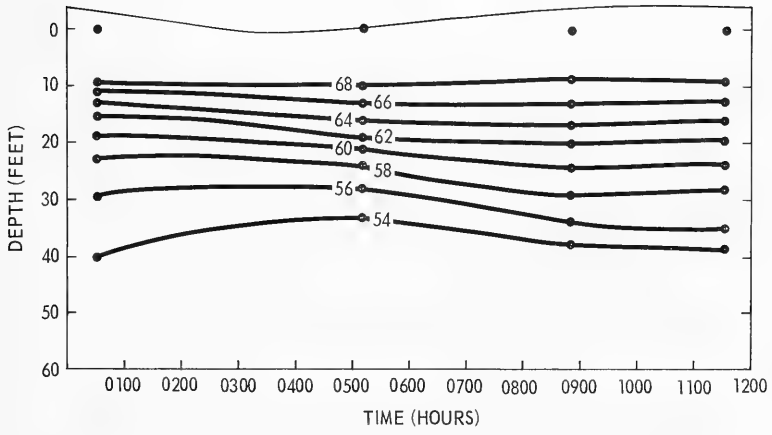

Figure A20. Water temperature (°F) 24 July 1964.

REVERSE SIDE BLANK

UNCLASSIFIED
Security Classification

DOCUMENT CONTROL DATA - R&D

(Security classification of title, body of abstract and indexing annotation must be entered when the overall report is classified)

1. ORIGINATING ACTIVITY *(Corporate author)*

U. S. Navy Electronics Laboratory
San Diego, California 92152

2a. REPORT SECURITY CLASSIFICATION
UNCLASSIFIED

2b GROUP

3. REPORT TITLE

PLANKTON AND TURBIDITY

4. DESCRIPTIVE NOTES *(Type of report and inclusive dates)*

Research and Development Report July 1961 to March 1966

5. AUTHOR(S) *(Last name, first name, initial)*

Barham, E. G., Wilton, J. W., and Sullivan, M. P.

6. REPORT DATE	7a. TOTAL NO. OF PAGES	7b. NO. OF REFS
1 July 1966	81	19

8a. CONTRACT OR GRANT NO.	9a. ORIGINATOR'S REPORT NUMBER(S)
b. PROJECT NO. SR 104 03 01, Task 0588 (NEL L40961)	1386
c.	9b. OTHER REPORT NO(S) *(Any other numbers that may be assigned this report)*
d.	

10. AVAILABILITY/LIMITATION NOTICES

Distribution of this document is unlimited.

11. SUPPLEMENTARY NOTES	12. SPONSORING MILITARY ACTIVITY
	Naval Ship Systems Command Department of the Navy

13. ABSTRACT

An investigation of time and space distribution of microorganisms and other materials producing attenuation of light in the open sea. Unicellular organisms in bloom quantities are found to reduce transmission of yellow light. Dinoflagellates are especially important during the summer off Mission Beach, California. Light transmission is also reduced by organic material, particulate detritus, and dissolved pigments. Macroplankton are found to be less important contributors.

DD FORM 1 JAN 64 1473 0101-807-6800

UNCLASSIFIED
Security Classification

14 KEY WORDS	LINK A		LINK B		LINK C	
	ROLE	WT	ROLE	WT	ROLE	WT
Microorganisms						
Oceans - Light Transmission						

INSTRUCTIONS

1. ORIGINATING ACTIVITY: Enter the name and address of the contractor, subcontractor, grantee, Department of Defense activity or other organization *(corporate author)* issuing the report.

2a. REPORT SECURITY CLASSIFICATION: Enter the overall security classification of the report. Indicate whether "Restricted Data" is included. Marking is to be in accordance with appropriate security regulations.

2b. GROUP: Automatic downgrading is specified in DoD Directive 5200.10 and Armed Forces Industrial Manual. Enter the group number. Also, when applicable, show that optional markings have been used for Group 3 and Group 4 as authorized.

3. REPORT TITLE: Enter the complete report title in all capital letters. Titles in all cases should be unclassified. If a meaningful title cannot be selected without classification, show title classification in all capitals in parenthesis immediately following the title.

4. DESCRIPTIVE NOTES: If appropriate, enter the type of report, e.g., interim, progress, summary, annual, or final. Give the inclusive dates when a specific reporting period is covered.

5. AUTHOR(S): Enter the name(s) of author(s) as shown on or in the report. Enter last name, first name, middle initial. If military, show rank and branch of service. The name of the principal author is an absolute minimum requirement.

6. REPORT DATE: Enter the date of the report as day, month, year; or month, year. If more than one date appears on the report, use date of publication.

7a. TOTAL NUMBER OF PAGES: The total page count should follow normal pagination procedures, i.e., enter the number of pages containing information.

7b. NUMBER OF REFERENCES: Enter the total number of references cited in the report.

8a. CONTRACT OR GRANT NUMBER: If appropriate, enter the applicable number of the contract or grant under which the report was written.

8b, 8c, & 8d. PROJECT NUMBER: Enter the appropriate military department identification, such as project number, subproject number, system numbers, task number, etc.

9a. ORIGINATOR'S REPORT NUMBER(S): Enter the official report number by which the document will be identified and controlled by the originating activity. This number must be unique to this report.

9b. OTHER REPORT NUMBER(S): If the report has been assigned any other report numbers *(either by the originator or by the sponsor)*, also enter this number(s).

10. AVAILABILITY/LIMITATION NOTICES: Enter any limitations on further dissemination of the report, other than those imposed by security classification, using standard statements such as:

(1) "Qualified requesters may obtain copies of this report from DDC."

(2) "Foreign announcement and dissemination of this report by DDC is not authorized."

(3) "U. S. Government agencies may obtain copies of this report directly from DDC. Other qualified DDC users shall request through _____."

(4) "U. S. military agencies may obtain copies of this report directly from DDC. Other qualified users shall request through _____."

(5) "All distribution of this report is controlled. Qualified DDC users shall request through _____."

If the report has been furnished to the Office of Technical Services, Department of Commerce, for sale to the public, indicate this fact and enter the price, if known.

11. SUPPLEMENTARY NOTES: Use for additional explanatory notes.

12. SPONSORING MILITARY ACTIVITY: Enter the name of the departmental project office or laboratory sponsoring *(paying for)* the research and development. Include address.

13. ABSTRACT: Enter an abstract giving a brief and factual summary of the document indicative of the report, even though it may also appear elsewhere in the body of the technical report. If additional space is required, a continuation sheet shall be attached.

It is highly desirable that the abstract of classified reports be unclassified. Each paragraph of the abstract shall end with an indication of the military security classification of the information in the paragraph, represented as *(TS)*, *(S)*, *(C)*, or *(U)*.

There is no limitation on the length of the abstract. However, the suggested length is from 150 to 225 words.

14. KEY WORDS: Key words are technically meaningful terms or short phrases that characterize a report and may be used as index entries for cataloging the report. Key words must be selected so that no security classification is required. Identifiers, such as equipment model designation, trade name, military project code name, geographic location, may be used as key words but will be followed by an indication of technical context. The assignment of links, roles, and weights is optional.

Navy Electronics Lab., San Diego, Calif.
Report 1386

UNCLASSIFIED

PLANKTON AND TURBIDITY, by E. G. Barham, J. W. Wilton, and M. P. Sullivan, 81 p., 1 Jul 66.

An investigation of time and space distribution of microorganisms and other materials producing attenuation of light in the open sea. Unicellular organisms in bloom quantities are found to reduce transmission of yellow light. Dinoflagellates are especially important during the summer off Mission Beach, California. Light transmission is also reduced by organic material, particulate detritus, and dissolved pigments. Macroplankton are found to be less important contributors.

1. Microorganisms
2. Oceans - Light Transmission

I. Barham, E. G.
II. Wilton, J. W.
III. Sullivan, M. P.

SR 104 03 01, Task 0588
(NEL L40961)

This card is UNCLASSIFIED

Navy Electronics Lab., San Diego, Calif.
Report 1386

UNCLASSIFIED

PLANKTON AND TURBIDITY, by E. G. Barham, J. W. Wilton, and M. P. Sullivan, 81 p., 1 Jul 66.

An investigation of time and space distribution of microorganisms and other materials producing attenuation of light in the open sea. Unicellular organisms in bloom quantities are found to reduce transmission of yellow light. Dinoflagellates are especially important during the summer off Mission Beach, California. Light transmission is also reduced by organic material, particulate detritus, and dissolved pigments. Macroplankton are found to be less important contributors.

1. Microorganisms
2. Oceans - Light Transmission

I. Barham, E. G.
II. Wilton, J. W.
III. Sullivan, M. P.

SR 104 03 01, Task 0588
(NEL L40961)

This card is UNCLASSIFIED

Navy Electronics Lab., San Diego, Calif.
Report 1386

UNCLASSIFIED

PLANKTON AND TURBIDITY, by E. G. Barham, J. W. Wilton, and M. P. Sullivan, 81 p., 1 Jul 66.

An investigation of time and space distribution of microorganisms and other materials producing attenuation of light in the open sea. Unicellular organisms in bloom quantities are found to reduce transmission of yellow light. Dinoflagellates are especially important during the summer off Mission Beach, California. Light transmission is also reduced by organic material, particulate detritus, and dissolved pigments. Macroplankton are found to be less important contributors.

1. Microorganisms
2. Oceans - Light Transmission

I. Barham, E. G.
II. Wilton, J. W.
III. Sullivan, M. P.

SR 104 03 01, Task 0588
(NEL L40961)

This card is UNCLASSIFIED

Navy Electronics Lab., San Diego, Calif.
Report 1386

UNCLASSIFIED

PLANKTON AND TURBIDITY, by E. G. Barham, J. W. Wilton, and M. P. Sullivan, 81 p., 1 Jul 66.

An investigation of time and space distribution of microorganisms and other materials producing attenuation of light in the open sea. Unicellular organisms in bloom quantities are found to reduce transmission of yellow light. Dinoflagellates are especially important during the summer off Mission Beach, California. Light transmission is also reduced by organic material, particulate detritus, and dissolved pigments. Macroplankton are found to be less important contributors.

1. Microorganisms
2. Oceans - Light Transmission

I. Barham, E. G.
II. Wilton, J. W.
III. Sullivan, M. P.

SR 104 03 01, Task 0588
(NEL L40961)

This card is UNCLASSIFIED

INITIAL DISTRIBUTION LIST

CHIEF OF NAVAL MATERIAL
MAT033
COMMANDER, NAVAL SHIP SYSTEMS COMMAND
SHIPS 1610
SHIPS 1620
SHIPS 2021 (2)
SHIPS 204113
COMMANDER, NAVAL SHIP ENGINEERING CENTER
CODE 6420
CODE 6440
CODE 6452E
CODE 6454
COMMANDER, NAVAL ORDNANCE SYSTEMS COMMAND
DLI-3
DLI-304
FASS
R-56
RU-222
RUDC
RUDC-2
RUDC-3
CHIEF OF NAVAL PERSONNEL
PERS 11B
CHIEF OF NAVAL OPERATIONS
OP-312F
OP-07T
OP-071
OP-71
OP-03EG
OP-09B5
OP-311
OP-322C
OP-702C
OP-716
OP-922Y4C1
CHIEF OF NAVAL RESEARCH
CODE 416
CODE 418
CODE 427
CODE 466
CODE 468
CODE 493
COMMANDER IN CHIEF US PACIFIC FLEET
COMMANDER IN CHIEF US ATLANTIC FLEET
COMMANDER OPERATIONAL TEST AND EVALUATION FORCE
DEPUTY COMMANDER OPERATIONAL TEST AND EVALUATION FORCE, PACIFIC
COMMANDER SUBMARINE FORCE
US PACIFIC FLEET
US ATLANTIC FLEET
DEPUTY COMMANDER SUBMARINE FORCE, US ATLANTIC FLEET
COMMANDER ANTISUBMARINE WARFARE FORCE US PACIFIC FLEET
COMMANDER FIRST FLEET
COMMANDER SECOND FLEET
COMMANDER TRAINING COMMAND US ATLANTIC FLEET
OCEANOGRAPHIC SYSTEM PACIFIC
COMMANDER SUBMARINE DEVELOPMENT GROUP TWO
COMMANDER KEY WEST TEST AND EVALUATION DETACHMENT
DESTROYER DEVELOPMENT GROUP PACIFIC
FLEET AIR WINGS, ATLANTIC FLEET SCIENTIFIC ADVISORY TEAM
NAVAL AIR DEVELOPMENT CENTER
NADC LIBRARY
NAVAL MISSILE CENTER
TECH. LIBRARY
PACIFIC MISSILE RANGE /CODE 3250/ LIBRARY
NAVAL ORDNANCE LABORATORY
SYSTEMS ANALYSIS GROUP OF THE ASW RESEARCH AND DEVELOPMENT PLANNING COUNCIL
CODE RA
NAVAL ORDNANCE TEST STATION
PASADENA ANNEX LIBRARY
CHINA LAKE
NAVAL WEAPONS LABORATORY
KXL
LIBRARY
PEARL HARBOR NAVAL SHIPYARD
PORTSMOUTH NAVAL SHIPYARD
PUGET SOUND NAVAL SHIPYARD
SAN FRANCISCO NAVAL SHIPYARD
RADIOLOGICAL DEFENSE LABORATORY
DAVID TAYLOR MODEL BASIN
LIBRARY
NAVY MINE DEFENSE LABORATORY
NAVAL TRAINING DEVICE CENTER
CODE 365H, ASW DIVISION
UNDERWATER SOUND LABORATORY
LIBRARY
CODE 905
ATLANTIC FLEET ASW TACTICAL SCHOOL
NAVY MARINE ENGINEERING LABORATORY
NAVAL CIVIL ENGINEERING LABORATORY
L54
NAVAL RESEARCH LABORATORY
CODE 2027
CODE 5440
NAVAL ORDNANCE LABORATORY
CORONA
UNDERWATER SOUND REFERENCE LABORATORY
FLEET ASW SCHOOL
FLEET SONAR SCHOOL
NAVY UNDERWATER WEAPONS RESEARCH AND ENGINEERING STATION
OFFICE OF NAVAL RESEARCH
PASADENA
NAVAL SHIP MISSILE SYSTEMS ENGINEERING STATION
CHIEF OF NAVAL AIR TRAINING
WEATHER RESEARCH FACILITY
NAVAL OCEANOGRAPHIC OFFICE
SUPERVISOR OF SHIPBUILDING GROTON
NAVAL POSTGRADUATE SCHOOL
LIBRARY (CODE 0384)
FLEET NUMERICAL WEATHER FACILITY
NAVAL APPLIED SCIENCE LABORATORY
CODE 9200, ELECTRONICS DIVISION
CODE 9832
ASSISTANT SECRETARY OF THE NAVY RESEARCH AND DEVELOPMENT
NAVAL SECURITY GROUP HEADQUARTERS (G43)
ONR SCIENTIFIC LIAISON OFFICER
WOODS HOLE OCEANOGRAPHIC INSTITUTION
INSTITUTE OF NAVAL STUDIES
LIBRARY
AIR DEVELOPMENT SQUADRON ONE /VX-1/
SUBMARINE FLOTILLA ONE
DEFENSE DOCUMENTATION CENTER (20)
DOD RESEARCH AND ENGINEERING WEAPONS SYSTEMS EVALUATION GROUP
DEFENSE ATOMIC SUPPORT AGENCY
FEDERAL COMMUNICATIONS COMMISSION
ABERDEEN PROVING GROUND
REDSTONE SCIENTIFIC INFORMATION CENTER
ARMY ELECTRONICS RESEARCH AND DEVELOPMENT LABORATORY, AMSEL-RD-MAT
COASTAL ENGINEERING RESEARCH CENTER
CORPS OF ENGINEERS, US ARMY
AFRSTA
HEADQUARTERS, US AIR FORCE
AIR UNIVERSITY LIBRARY
AIR PROVING GROUND CENTER, PGEPS-12
HQ AIR WEATHER SERVICE
WRIGHT-PATTERSON AF BASE
SYSTEMS ENGINEERING GROUP (RTD)